Optimization of Exhaust Aftertreatment Systems using CFD

Master Thesis

University of Rostock
Faculty of Mechanical Engineering and Ship building, Chair of Modelling and Simulations

Scania Technical Center
Department of Exhaust Aftertreatment Systems, Engine Exhaust Performance Simulations (NXPS)

Industrial Supervisor: Louis Carbonne
CFD-Internal Flow & HVAC Engineer | Truck Chassis Development, NXPS, STC, Scania CV AB, Södertälje, Sweden.

Academic Supervisor: Prof. Dr. Ing. Habil. Nikolai Kornev
Chair at Modelling and Simulations, University of Rostock, Germany.

Student: Atul Singh
Matrikel Number: 216100191

Statement of Authorship

I hereby certify that this master thesis has been composed by myself, and describes my own work, unless otherwise acknowledged in the text.
All references and verbatim extracts have been quoted, and all sources of information have been specifically acknowledged. It has not been accepted in any previous application for a degree.

Atul Udaivir Singh.
University of Rostock

Optimization of Exhaust Aftertreatment Systems using CFD

by

Atul Singh

Submitted to the Department of Modelling and Simulations at University of Rostock

for partial fulfillment of the requirements for the

Masters of Science in Computational Science and Engineering

Abstract

Strict emission norms for non renewable fuel based vehicles has led to continuous development and improvement of exhaust aftertreatment systems in the recent years. The developments here at Scania too, are directed towards the EU-6 emission norms which strive towards building less polluting and more efficient fuel consuming vehicles then their previous versions. In this endeavour, a multi disciplinary research and development cycles focused exclusively to reduce emissions, reduce fuel consumption, and increase sound reduction is desirable. The current method used by Scania, of finding out such best performing or most optimal configurations out of the various possibilities, is both resource and time intensive.

The current work aims towards building an easier and fungible way of conducting such studies. An Exhaust aftertreatment subsystem is used as a test case to develop this optimization study for CFD performance. Three objective functions of minimizing pressure drop, maximizing flow uniformity of exhaust gasses in this subsystem and minimizing wall film mass in this exhaust system, are looked at. (Wall films are developed at the surface of this exhaust sub system as a consequence of chemical reactions which attempt to reduce NOx emissions). Three different optimization methods are studied with various number of evaluations. Their results are compared to suggest a best approach given the number of objective functions at hand. Response surface modelling on these three optimization methods is also briefly studied. It is suggested that building a simple Design of experiments model on few evaluations based on surface uniformity objective function, seems to give much insight on the design space, than having pressure drop as the objective function. Furthermore, the more number of already existing designs used for building the approximation, the higher the chance of finding an approximation accuracy reducing design (outliers). It is also suggested that, by using some of the first evaluations out of all of them, the approximation is still not better than the original sampling, however, the relative difference is comparatively close. Best designs from original evaluations and approximated evaluations are compared.

Keywords :- Optimization, CFD, Exhaust Aftertreatment Systems, Design of Experiments, Response surface Modelling, Kriging, STAR-CCM+, AVL-FIRE, HEEDS.

Acknowledgments

I would like to thank my industrial supervisor at Scania CV, Mr Louis Carbonne, for believing in me by giving this opportunity, guiding me, and most importantly, encouraging me at every step of the way during my time at Scania. I have picked up many good things from him, not only as an engineer, but also as a person. All of which I am going to deeply cherish for the rest of my life.

I sincerely thank other team members at NXPS in Scania CV who have been a group of closely knit amazing individuals and have always welcomed me in their team. It is because of them, I have now the taste of how an ideal team should feel like, both, to work, and to be around with. I have also to thank, Mr David Norrby and my manager Mr Kim Pettersson, who gave me this wonderful opportunity in the first place.

I have my sincerest gratitude for Professor Nikolai Kornev, whose teachings were most useful during the course of this work. It was his encouragement to me in my the second semester itself, that pushed me to secure this opportunity.

Lastly, I would like to thank my parents for being the core foundations of my moral support. They are to this day, making me understand the ways of cosmic spectrum and its essence, way better than anyone or anything ever could. My brother Mr Ashwin Singh and sister Mr Shilpi Saboo, who are always there for me whenever I need them, few questions asked. And to my friends ofcourse, especially, Mr Parth Tripathi, Mr Sudhanva Chandrashekhara, Mr Onkar Jadhav, Mr Ujjwal Verma, and Mr Lohith Bheemiah. whose presence, I have realized, is nothing short of a gift from the divine.

Nomenclature

Acronyms

NXPS	Engine Exhaust Performance Simulation
STC	Scania Technical Centre
DoE	Design of Experiments
RSM	Response Surface Methodology
EAS	Exhaust Aftertreatment System
NO	Nitric Oxide
NO_2	Nitric di Oxide
SO_2	Sulphur di Oxide
HC	Hydro carbons
CO	Carbon mono Oxide
DOC	Diesel Oxidation Catalyst
DPF	Discrete Particulate Filter
SCR	Selective Catalytic Reductor
ASC	Ammonia Slip Catalyst
CSF	Coated Soot Filter
CFD	Computational Fluid Dynamics
FEM	Finite Element Methods
MO	Multi objective
WS	Weighted Sum
CAD	Computer Aided Design
DDM	Discrete Droplet Method
LHS	Latin Hypercube Sampling

Subscripts

b	body
u	user source term
f	face
t	total
abs	absolute
ref	reference
s	static
ext	extrapolated
i	incomming
d, p	droplet, particle
m	wall

Contents

1 Introduction **1**
1.1 Background . . . 1
1.2 Purpose . . . 3
1.3 Objectives . . . 3
1.4 Limitations . . . 4

2 Theory **5**
2.1 Aftertreatment System . . . 5
2.2 Evaporation unit . . . 6
2.2.1 Reactions . . . 7
2.2.1.1 Urea evaporation . . . 7
2.2.1.2 Wallfilm and solid deposits . . . 7
2.3 Computational Fluid Dynamics . . . 8
2.3.1 CFD with STAR-CCM+ . . . 8
2.3.1.1 Mechanics . . . 8
2.3.1.2 Surface Uniformity . . . 10
2.3.1.3 Pressure Drop . . . 10
2.3.2 CFD with AVL FIRE™ . . . 11
2.3.2.1 Spray module . . . 12
2.3.2.1.1 Basics of Spray Module . . . 12
2.3.2.1.2 SCR Evaporation submodel with Thermolysis . . . 13
2.3.2.1.3 Kuhnke/Wruck Wall Interaction and Wall Heat Transfer Subodels . . . 14
2.3.2.2 Wallfilm module . . . 15
2.3.2.2.1 Film Velocity Profiles . . . 16
2.3.2.3 Thin walls module . . . 16
2.4 Optimization with HEEDS . . . 17
2.4.1 Basic Terminologies . . . 17
2.4.2 Weighted Sum Parameter Optimization . . . 22
2.4.3 Multi Objective Parameter Optimization . . . 22
2.4.4 Response Surface Methods . . . 22

3 Method **25**
3.1 General Setup . . . 25
3.1.1 Windows and Linux connection . . . 25

3.1.2 Resources settings . . . 26
3.1.3 HEEDS Settings . . . 26
3.1.4 Softwares . . . 26
3.1.4.1 CATIA V5 . . . 26
3.1.4.2 ANSA . . . 27
3.1.4.3 STAR-CCM+ . . . 27
3.1.4.4 AVL-FIRE™ . . . 27
3.1.4.5 HEEDS . . . 27
3.2 STARCCM+ with HEEDS . . . 28
3.2.1 Methodology . . . 28
3.3 AVL FIRE™ with HEEDS . . . 30
3.3.1 Methodology . . . 30

4 Results and Discussion **32**
4.1 Flow analysis with STAR-CCM+ . . . 33
4.1.1 Design of Experiments/Screening Response . . . 33
4.1.1.1 Response Surface for DoE Study . . . 35
4.1.1.2 Surrogate for DoE Study . . . 36
4.1.2 Multi Objective Parameter Optimization . . . 40
4.1.2.1 Response surface for Multi Objective Study . . . 43
4.1.2.2 Surrogate for Multi Objective Study . . . 45
4.1.3 Weighted Sum Objective Parameter Optimization . . . 49
4.1.3.1 Response surface for Weighted Sum Study . . . 50
4.1.3.2 Surrogate for Weighted Sum Study . . . 52
4.1.4 Verification . . . 56
4.2 Spray CFD with AVL FIRE . . . 57
4.2.1 Multi Objective Parameter Optimization . . . 58

5 Conclusions **64**
5.1 Future Work . . . 66

Bibliography **67**

List of Figures

1 European Union Emission Standards 2

2 EAS Schematic 5
3 Scania Silencer cutout for 6 cylinder engine for EU-6. [4] 6
4 Regime map for Spray wall interaction according to Kuhnke[18] . . 15
5 3 Possibilities between Design A and B with both objectives to be minimized 19
6 3 Ranks, along with the best ranks indicating a pareto front 20

7 STAR-CCM+ setup with HEEDS 28
8 AVL FIRE™ setup with HEEDS 30

9 Correlation between all involved parameters with the response . . . 33
10 Cross validation of Kriging response of SU_023 residual plotted against Kriging response of SU_023 36
11 Objective history of surrogate plotted with original 50 evaluations. . 37
12 Objective history for RSM cupdraft angle with original 50 evaluations. 38
13 Objective history for RSM cone angle difference obtained with original 50 evaluations. 38
14 3D response curve for 2 parameters for Kriging response of SU_023. 39
15 Pareto Plot showing design trade offs between pressure drop and surface uniformity 40
16 Radial plot for non error and top 30 designs 42
17 Surface uniformity plotted with Pressure drop to observe the variation between the two objective function value distribution. 43
18 Cross V residuals plotted against obtained Pressure drop values . . 44
19 Cross V residuals plotted against obtained Surface Uniformity drop values 45
20 Response surface pressure drop and surface uniformity, indicated with rank of designs 46
21 An inset to the optimal region of figure 20 46
22 Comparison between Surrogate and Original model 47
23 Pareto Plot for weighted sum objective study between pressure drop and surface uniformity 49
24 Radial plot for non error with top 30 designs for Weighted sum study. 50

25 Cross V residuals plotted against kriging response Pressure drop values. 51
26 Cross V residuals plotted against obtained kriging response Surface Uniformity values . . . 52
27 Surrogate for Responses obtained from first 100 design evaluations . 53
28 Zoomed inset for the 1000 evaluations . . . 53
29 Design space comparison between the 250 and 1000 evaluations highlighted by first 100 evaluations . . . 54
30 Response surface indicating the global minima with best original 30 designs . . . 55
31 Correlation plot for AVL-FIRE™ study . . . 57
32 Pressure Drop plotted against Wallfilm mass ranked with Surface uniformity . . . 58
33 Pressure Drop plotted against Wallfilm mass with the surrogate response . . . 59
34 Pressure Drop plotted against Surface uniformity ranked with wall film mass . . . 59
35 Inset of figure 34 indicating the Uniformity index of two designs out of the 58 . . . 60
36 Pressure Drop plotted against surface uniformity with the surrogate response . . . 61
37 Wallfilm mass plotted against Surface Uniformity ranked with pressure drop . . . 62
38 Wallfilm mass plotted against surface uniformity with the surrogate response . . . 62

List of Tables

1 Modelling settings for DoE Study 35
2 The mean value of the surrogate response, obtained from the training and test sets as defined in section 2.4.1 35
3 Response approximation values for Multi objective study 43
4 Cross Validation values compared for both objective functions for Multi objective study 44
5 Response approximation values for Weighted Sum study. 50
6 Cross Validation values compared for both objective functions . . . 51
7 Best design of Surrogate, simulated from the best responses for multi objective parameter optimization study 56
8 Best design of Surrogate, simulated from the best responses for Weighted Sum parameter optimization study 56
9 Comparison of best designs from original evaluations of 3 optimization methods 64

Chapter 1

Introduction

The aim of this chapter is to initiate reader towards describing the current thesis which was conducted at Scania CV AB. This chapter is outlined to give a brief idea about the company and the team, followed by purpose to perform such a study, aims of this work and finally, limitations for the same.

1.1 Background

Scania is a truck manufacturing company, with business operations in more than 100 countries, and more than 10.184 billion SEK (as of 2016) operating income which is steadily increasing. It is quickly moving towards being a complete transport solutions provider to various industries such as agriculture, constructions, military, retail, manufacturing, forestry, mining, petrochemicals etc. It's other products in its portfolio, apart from trucks and busses, include, Marine engines, power generators, Long haul trucks and fleet management systems. Scania is also driving the autonomous wave as well as other ground breaking solutions such as platooning, that helps its fleet management solutions. The heart of all this development is based at STC located in Södertälje, Sweden, where the current study was conducted.

The Thesis was conducted at the NXPS department of Scania Technical Center. This focused group deals with the Aftertreatment system performance and simulations using CFD and Acoustics as its major disciplines. Conducting simulations to verify a new design or improve the existing ones, forms the day to day activities of this group, among many other things. The simulations, like this study, could vary from flow simulations, to spray simulations, as well as those keeping with only acoustic performance as its core focus.

A complex product such as the aftertreatment systems, requires careful development as it is directly related to the fuel consumption of the vehicle as well as to the gasses it emits. Add to this, the increasing competition and strict emission norms which has given enough incentives to development teams to find better, quick and efficient solutions for their product development cycles.

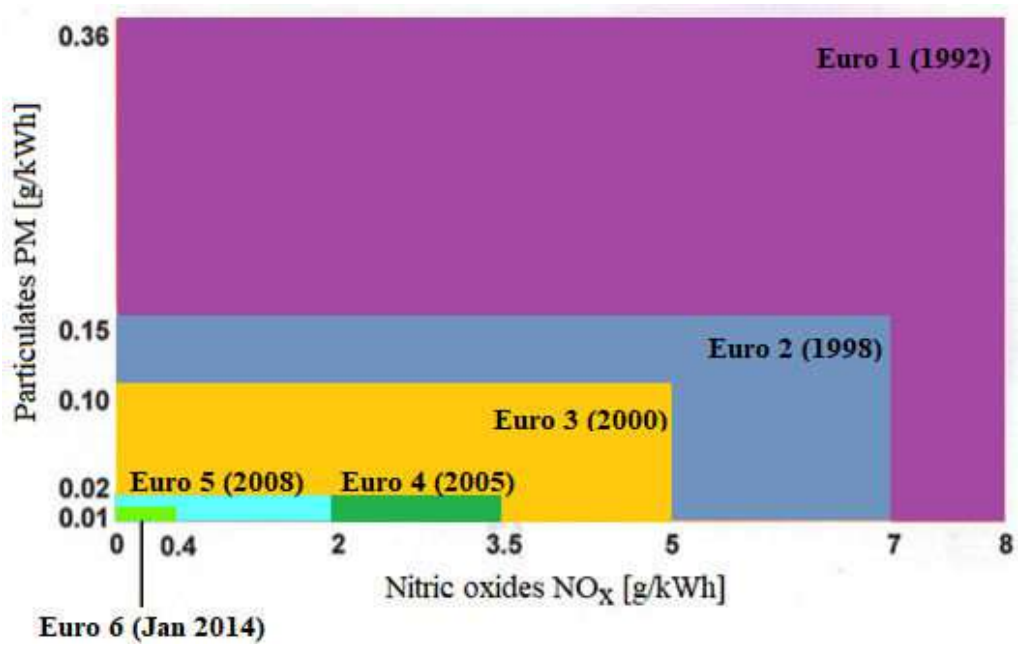

Figure 1: European Union Emission Standards

A comparison of emission regulations spread across the years is shown in figure 1. Although this has been the case for quite a while now, developing new methods to help reach this emission standard quickly, through it's development processes, would not only help Scania decrease its development time but also increase its revenue. It stands to reason that with Paris climate agreement in place [1], among other emission regulations, this condition is only going to be made stricter. Also, Scania as a corporate truck manufacturer always strives to improve it's development cycles, a vision to which this thesis tries to contribute to.

The scope and work of this thesis, then aims to contribute to the method in which this group (NXPS) performs its optimization studies with CFD for both flow and spray simulations. These are two major classification of CFD simulations that are conducted within NXPS. A strong focus on design of experiments as well as optimization of it's exhaust systems is kept. This method is also supposed to be seamlessly integrated and adopted by the other subsidiary, parallel, dependent simulation departments within Scania. Other departments too, should be able to replicate this method with ease, assuming they too conduct optimization on similar softwares as used in the current study. The fungibility of the proposed method is a desired aspect, even if the applications studied were other than that of CFD, like Acoustics or FEM analysis for instance. Hence it becomes important, that other engineers can replicate it with minimum involvement and investment of their time and resources.

1.2 Purpose

The exhaust systems division at Scania conducts Design of Experiments and Optimization (former more than the later) analysis on a daily basis. It mainly uses following softwares for them, from perspective of CFD performance.

- STAR-CCM+
- AVL FIRE™
- OpenFOAM

Some of the other assisting, yet still extensively used softwares being

- CATIA V5
- ANSA

CATIA V5 functions as a CAD Tool while ANSA as the meshing software to conduct these studies. So, given the depth and frequency with which Design of Experiments and Optimization is conducted at NXPS, it only stands to reason that it should be able to integrate and couple all or most of these softwares under one workflow in order to conduct them in an efficient and less time consuming manner. This is developed with another software of HEEDS which is a commonly used tool in the industry. This software builds upon integrating the already used softwares at NXPS for conducting Design of Experiments and Optimization, which were previously done with a lot of manual scripting using excel sheets and other such subsidiary tools. Another added advantage of this software is it's post processing abilities, which is why NXPS is investing time to derive value out of this tool.

The proposed method not only saves time, but also aims to increases the engineer's time on development issues rather than setup issues. A then "nice to haves" from this interface or workflow, would be the obtained DoE and Optimization results, which can give a sense of comparison of how the suggested method improves on the already persisting methods at this team.

1.3 Objectives

The aims of this thesis are

- To develop Optimization and Design of Experiments method in HEEDS for the EAS subsystem with internal flow CFD performed with STAR-CCM+
- To investigate and understand which parameters affect the internal flow of the evaporation unit, and how they are linked to the defined objective functions of surface uniformity, pressure drop as well as wall film mass for the same.


- To explore Response surface methodologies,(surrogate modelling, meta modelling), within the capabilities of HEEDS, to see if they offer any insights apart from the original design space.
- To build an optimization method for spray CFD in HEEDS conducted using AVL FIRE™
- To investigate and obtain the most feasible designs for AVL FIRE™ optimization, defined with 3 objective functions.

The term Multi Disciplinary Optimization (MDO) comes into play here as there are two different focus for this workflow, i.e Flow and Spray simulations. Another desirable aspect of this method is the fungibility with which it can be replicated for other studies in other departments within Scania.

1.4 Limitations

The core focus of the current study is to develop optimization methods and not the calibration or improvement of either spray, nor flow characteristics for its CFD aspect. The configurations related to CFD for both, internal flow simulation with STAR-CCM+ and spray simulations with AVL-FIRE™ have been taken as is, following Scania's own protocol to conduct these studies. Hence these are also not discussed in the current study because of the confidentiality clause associated with this work. The method to integrate all the softwares mentioned in section1.2 forms the central aspect of the current thesis. However results too are discussed in some detail to demonstrate the capabilities of the suggested method to other teams at Scania.

It was also required to have simple CFD models with not too many cells, as the nature of this thesis required so. The setup phase requires to first build a functional workflow, before performing any fine tuning to it. Which is why, the STAR-CCM+ run is for only 100 steps for a steady state condition with 2M cells mesh size, while the AVL-FIRE™ study is for slightly heavy mesh of 6M cells. Also, the transient simulation data generated from the spray simulation setup is for only 1 second, which is too low, to make any conclusive design decision.

Chapter 2

Theory

A brief theoretical background is given for all the concepts that should be used to understand the results obtained from the current work. As the current work spans the concepts ranging from Automotive, CFD, and Optimization, they are touched upon briefly in this chapter one by one.

2.1 Aftertreatment System

A simple schematic of an Scania EAS is shown in figure 2. This gives a clear indication of the systems and units that belong to any general aftertreatment systems, give or take a few things. This model, is however good representation for the current study.

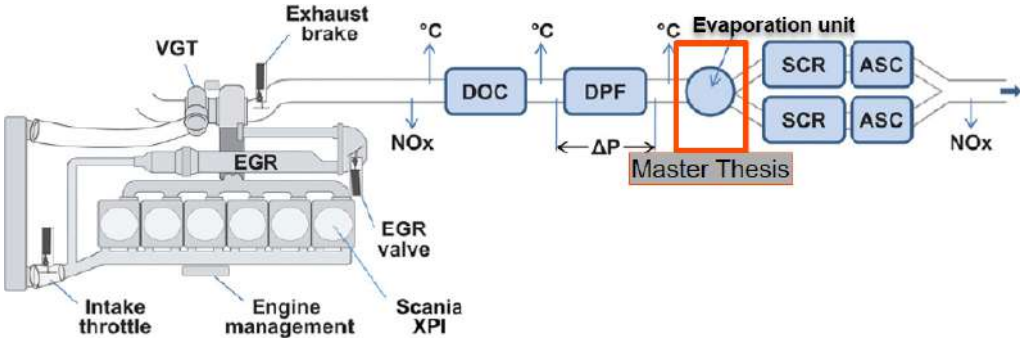

Figure 2: EAS Schematic

Engine exhaust manifold (pipe before DOC), contains combustion exhaust gasses with all the by products of emissions inside of it. The main functions of all the individual units inside this system is given as follows.

- The DOC primarily functions to oxidize Carbon monoxide and Hydrocarbons, but SO_2 and NO are also oxidized to a certain extent within this unit.[2]
- The DPF then takes these as input and oxidizes NO, HC, and CO and temporarily store soot for later oxidation. This unit also collects ash to keep particulate emission below thresholds.

- The mixture now obtained is injected with Urea in the Evaporation unit. This is done with Adblue® which is a 32.5% Ammonia solution. This is done to obtain gaseous NH_3 that is required downstream in the SCR to react with the NOx present in the system. Adblue® is injected from a different vessel attached to the truck chassis externally, at the interface of DPF and Evaporation unit.
- The SCR then, is responsible for producing only N_2 and H_2O, before leaving the exhaust system, which are not harmful for the human respiratory system. [3]
- ASC then oxidizes remaining Ammonia from the stream (as Ammonia is harmful for the humans, and should be taken care of)

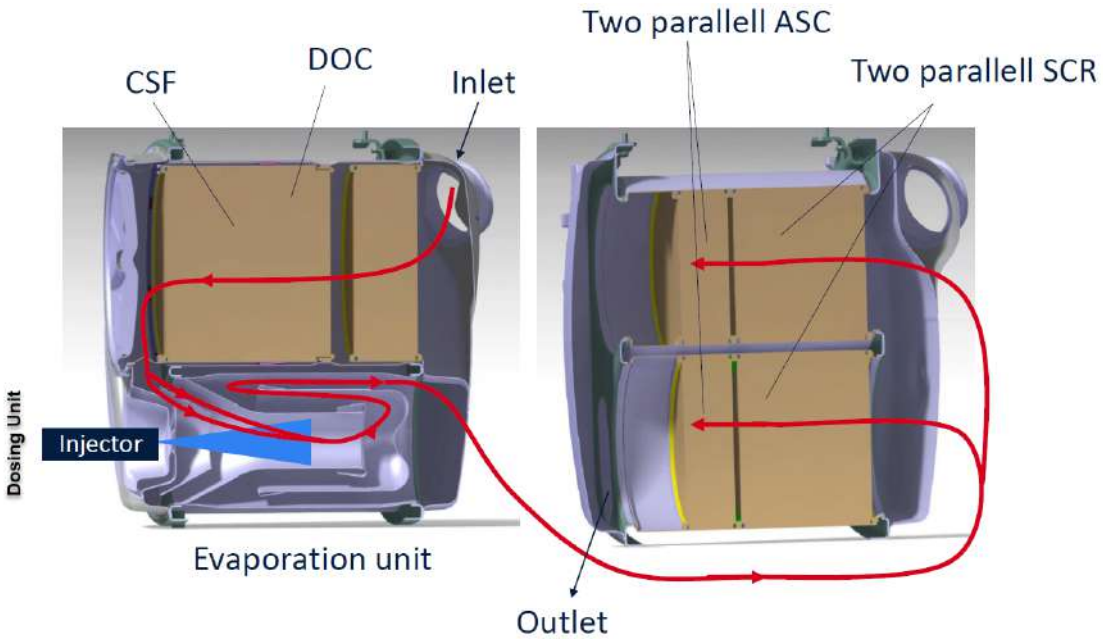

Figure 3: Scania Silencer cutout for 6 cylinder engine for EU-6. [4]

A more precise flow direction is depicted in the figure 3 system cutout. Here flow can be seen to follow across all the unit of the exhaust, with each respective units performing their respective chemical/surface reactions in them. The arrangement of an external injector forming a dosing unit, used to spray the Adblue® to the evaporation unit can also be seen.

2.2 Evaporation unit

Evaporation module comprises of two concentric tubes, separated by a corrugation of metallic fins in the annulus region. The gasses are entering it from the DOC and DPF where they continue towards the SCR and ASC. (All of which remain

out of the scope for the current study). There is a mixing fan to increase mixing of ammonia in the exhaust gases, so that the swirl of the flow could be increased, hence aiding in the mixing of chemical reactions involved. Here, the annulus structure of the evaporation unit facilitates sufficient heat transfer between the surfaces (the flow reversing in the evaporation unit, before reaching into two parallel SCR in figure 3), as the flow is made to pass in both of them. This makes the inner walls of the evaporation unit hot enough for the ammonia to evaporate as soon as it is splashed onto it (equation 2.1). The bigger area the Adblue® sprays onto, the better the evaporation rate is achieved.

2.2.1 Reactions

Some chemical reactions specific to the Evaporation unit is shown as follows.

2.2.1.1 Urea evaporation

Internal Combustion engines are always ridden with exhaust gasses containing harmful matter for the environment. Nitrogen oxides (NO_2) and Nitric oxides(NO) form these gasses collectively known as NOx.[5]

The Adblue® acts as the hydrolysis agent for the following reactions.[6]

$$(NH_2)_2CO \bullet 7H_2O \longrightarrow (NH_2)_2CO + 7H_2O \tag{2.1}$$

$$(NH_2)_2CO \longrightarrow HCNO + NH_3 \tag{2.2}$$

$$HCNO + H_2O \longrightarrow CO_2 + NH_3 \tag{2.3}$$

The above reactions forms the Evaporation, Thermolysis and Hydrolysis reactions within the Evaporation unit respectively. Isocyanic acid (HCNO) generated in equation 2.2 is disintegrated into Ammonia NH_3 and H_2O in the subsequent hydrolysis reaction in equation2.3

This Ammonia obtained in equation 2.3 is then used to reduce the remaining NOx present in the system, downstream with the SCR unit.

2.2.1.2 Wallfilm and solid deposits

It is important to note the formation of wall films and solid deposits, at the evaporation unit mainly because of the operating conditions that end up favouring the crystallization process i.e., if the evaporation performance is not upto the mark, there is a risk of creating solid deposits. It is difficult to know under which conditions solid deposits are created, but they usually appear when walls become cold, which creates wall films and then these films are transported to places where it will remain stagnant. Accumulation of such deposits leads to a decrease in pressure drop performance and increase the fuel consumption of the vehicle. This necessitates the need to understand this phenomena of development of wall films in order to device

methods to minimize it.

If Adblue® remains in higher quantities in the unit, there are higher chances of the film formation and solid deposits, leading to a poor evaporation performance. While if the mixing performance is not adequate, the Ammonia required downstream would be inadequate[7] leading to a low NOx conversion performance. These both have the potential to decreases the overall performance of the aftertreatment system along with other durability issues. [8]

2.3 Computational Fluid Dynamics

CFD basics are employed with help of two softwares as mentioned in section 1.2, namely STAR-CCM+ and AVL FIRE™ and are discussed briefly in this section. For CFD basics themselves, the reader is referred to [9], [10], [11].

2.3.1 CFD with STAR-CCM+

STAR-CCM+ offers attractive capabilities for conducting CFD and this is the reason it is currently an industry standard because of its solver, as well as post processing prowess. The current section delves into the basics of the equations it uses, in order to reach to the results discussed within the scope of the current work.

2.3.1.1 Mechanics

All of the equations discussed in this sections are explained in the context of STAR-CCM+ [12].
Mass balance in a control volume is expressed by continuity equation

$$\frac{\partial \rho}{\partial t} + \nabla \cdot (\rho \mathbf{v}) = 0 \tag{2.4}$$

here ρ is density and v is continuum velocity. The time rate change of linear momentum is the resultant force acting on the continuum given as follows.

$$\frac{\partial (\rho \mathbf{v})}{\partial t} + \nabla \cdot (\rho \mathbf{v} \otimes \mathbf{v}) = \nabla \cdot \sigma + \mathbf{f}_b \tag{2.5}$$

where $\otimes$ denotes the outer product, f_b is the resultant of the body forces (such as gravity and centrifugal forces) per unit volume acting on the continuum, and σ is the stress tensor. For fluids, the stress tensor is often written as sum of normal stresses and shear stresses, $\sigma = pI + T$, where p is the pressure and T is the viscous stress tensor, giving:

$$\frac{\partial (\rho \mathbf{v})}{\partial t} + \nabla \cdot (\rho \mathbf{v} \otimes \mathbf{v}) = -\nabla \cdot (\rho \mathbf{I}) + \nabla \cdot \mathbf{T} + \mathbf{f}_b \tag{2.6}$$

The conservation of angular momentum needs a symmetric stress tensor defined as follows

$$\sigma = \sigma^T \tag{2.7}$$

while, the energy conservation applied to the control volume is written as:

$$\frac{\partial(\rho E)}{\partial t} + \nabla \cdot (\rho E \mathbf{v}) = \mathbf{f}_b \cdot \mathbf{v} + \nabla \cdot (\mathbf{v} \cdot \sigma) - \nabla \cdot \mathbf{q} + S_E \tag{2.8}$$

where E is the total energy per unit mass, q is the heat flux, and S_E is an energy source per unit volume.

Integrating equation 2.4, equation 2.6, and equation 2.8 over a finite control volume, the governing equations of fluid flow can be written as Continuity Equation (CE), Momentum Equation(MV), and Energy Equation (EE) as follows.

$$CE: \frac{\partial}{\partial t}\int_V \rho dV + \oint_A \rho \mathbf{v} \cdot d\mathbf{a} = \int_V S_u dV \tag{2.9}$$

$$MV: \frac{\partial}{\partial t}\int_V \rho \mathbf{v} dV + \oint_A \rho \mathbf{v} \otimes \mathbf{v} \cdot d\mathbf{a} = -\oint_A p\mathbf{I} \cdot d\mathbf{a} + \oint_A \mathbf{T} \cdot d\mathbf{a} + \int_V \mathbf{f}_b dV + \int_V \mathbf{s}_u dV \tag{2.10}$$

$$EE: \frac{\partial}{\partial t}\int_V \rho E dV + \oint_A \rho H \mathbf{v} \cdot d\mathbf{a} = -\oint_A \mathbf{q} \cdot d\mathbf{a} + \oint_A \mathbf{T} \cdot \mathbf{v} d\mathbf{a} + \int_V \mathbf{f}_b \cdot \mathbf{v} dV + \int_V S_u dV \tag{2.11}$$

S_u and s_u are user source terms.

Solving equation 2.10 for velocity, requires a closure between the stress tensor and the velocity field. This approach changes according to the material properties of the fluid, i.e viscosity, normal stress coefficient etc.

A Newtonian fluid is described by an explicit constitutive equation that relates the viscous stress tensor T to the velocity field through a constant viscosity.

$$D = \frac{1}{2}(\nabla \cdot v + (\nabla \cdot v)^T) \tag{2.12}$$

While the stress tensor is given by

$$T = 2\mu D - \frac{2}{3}\mu(\nabla \cdot v) \cdot I \tag{2.13}$$

where μ is the constant dynamic viscosity of the fluid and D is the rate of deformation (strain) tensor given by equation 2.12.

The viscous stress tensor in Equation 2.6 is not constant, but a variable function of the velocity field for a particular fluid. Typically, in a constitutive relation, the velocity field is expressed in the form of the rate of deformation tensor:

As this is an exhaust gas modelling with Newtonian fluid, the viscosity is modelled as a function of temperature with Sutherland's Law.

$$\frac{\mu}{\mu_0} = (\frac{T}{T_0})^{-3/2} \cdot (\frac{T_0 + S}{T + S}) \tag{2.14}$$

Here, S is called the Sutherland constant, and μ_0 is the reference viscosity at the reference temperature T_0=273K

2.3.1.2 Surface Uniformity

Surface uniformity forms an important objective function for the current thesis as well as from the perspective of an Evaporation unit. This is because of the requirement of maximizing evaporation performance as discussed in section 2.2 to which surface uniformity helps giving a quantitative comparison between the designs under scrutiny. The current study looks at this surface uniformity at the annulus region of the model, mentioned in section 2.2. This is done so, because a high uniformity in this area would mean more uniform heat transfer coefficient from the flow to the heat flanges, indicating a better evaporation condition within this system. Ideally it should be as high as possible for the current work. Hence it will be defined to be maximized in the objective definition for optimization.

The surface uniformity of a quantity [13] essentially describes the distribution of a certain quantity on a surface. If the quantity is distributed equally, the resulting number is 1. This report is useful in applications where a uniform flow rate is desired across a whole area. Heat exchangers, catalysts, and filters are examples of such applications.

This is calculated for a scalar as follows:

$$\phi = 1 - \frac{\left|\phi_f - \bar{\phi}\right| \cdot A_f}{2\left|\bar{\phi}\right| \sum_f A_f} \tag{2.15}$$

where where $\bar{\phi}$ is the surface average of ϕ and ϕ_f is the face value of the selected scalar and A_f is the area of a face. This study is mostly focused on discussing velocity uniformity, so $\phi = v$.

2.3.1.3 Pressure Drop

Pressure drop forms a more general performance criteria for the whole EAS since it has a direct correlation with the fuel consumption. It is desirable to have as minimum of pressure drop as possible. It is defined in STAR-CCM+ as follows.

$$dp = \left[\frac{\sum_f |\dot{m}_f| \, P_{t,abs_f}}{\sum_f |\dot{m}_f|}\right]_{high} - \left[\frac{\sum_f |\dot{m}_f| \, P_{t,abs_f}}{\sum_f |\dot{m}_f|}\right]_{low} \tag{2.16}$$

The report will calculate the mass-flow averaged absolute total pressure difference between two groups of boundary surfaces representing the high and low pressure boundaries of the system. $\dot{m}_f$ is the mass flow across a face, where $[P_{t,abs_f}]_{high}$ and $[P_{t,abs_f}]_{low}$ are the absolute total pressure on the faces of the input high pressure and low pressure boundary surfaces, respectively. The subset f represents face. The other terms in the above equation are shown as follows.

$$P_{t,abs_f} = P_t + P_{ref} \tag{2.17}$$

Here the Total absolute pressure on a face is defined as a sum of total and reference pressure, while the Total Pressure is given as

$$P_t = P_{abs}\left[\left(1 + \frac{(\gamma-1)}{2}\cdot M^2\right)^{\frac{\gamma}{(\gamma-1)}}\right] - P_{ref} \tag{2.18}$$

P_{ref}, P_{abs}, M, γ are reference pressure, absolute pressure, Mach number, and ratio of specific heats, respectively.
Similarly to obtain the mass flow rate for equation 2.16, STAR-CCM+ first calculates the following values at the boundary faces, namely

- velocity v
- Static Pressure P_s
- Static Temperature T_s

where P_s at the boundary is calculated as

$$P_s = \begin{cases} P_{spec} & \text{for subsonic flows} \\ P_s^{ext} & \text{for supersonic flows.} \end{cases} \tag{2.19}$$

Here, P_{spec} is the specified pressure and P_s^{ext} is the extrapolated pressure, from the interior of the domain.

Static Temperature T_s for non isothermal cases, is calculated as

$$T_s = T_s^{ext} \tag{2.20}$$

Finally, for the equation 2.16 the mass flow is calculated after specifying a mass flow rate for the inlet. STAR-CCM+ first distributes it over all faces and calculates a uniform mass flow rate on each face of the boundary.

$$\dot{m} = \dot{m}_{total,spec}\frac{|a|}{A} \tag{2.21}$$

where $\dot{m}_{total,spec}$ is the total mass flow rate, specified by the user, **a** is the outward pointing face area vector, and A is the total area of the boundary.

2.3.2 CFD with AVL FIRE™

The incentive to use this software is for the spray simulations as it has some advantages over STAR-CCM+ and is also used by NXPS frequently for this purpose. It is also a current industry standard for conducting state of the art combustion and spray modelling simulations. Few modules pertaining to it are briefly explained, relevant to the current study. Note that the basic CFD conservation principles defined above remains same, however, the difference will only be in the modules that are employed here apart from those used within STAR-CCM+.

2.3.2.1 Spray module

Spray simulation [14] involves multi-phase flow phenomena and as such requires a numerical solution of conservation equations for the gaseous and liquid phases simultaneously. Engineering applications with liquid phase problems mostly employ Discrete Droplet Method (DDM)[15].

This model operates by solving ODE's for the trajectory, momentum, heat and mass transfer of single droplets, each being a member of a group of identical non-interacting droplets termed as 'parcels'. Hence one member of the group will imitate complete parcel. Settings for these parcel are then set manually in AVL FIRE™.The basics of this model is discussed as follows.

2.3.2.1.1 Basics of Spray Module

For the trajectory and velocity of a particle parcel, differential equations are as follows [14]:
The momentum equation is given as,

$$m_d \frac{du_{id}}{dt} = F_{idr} + F_{ig} + F_{ip} + F_{ivm} + F_{ib} \tag{2.22}$$

Where F_{idr} is the drag force of the incoming droplet, given by,

$$F_{idr} = D_p \cdot u_{irel} \tag{2.23}$$

with u_{irel} as relative velocity of incoming droplet.
Here D_p is the drag function defined as,

$$D_p = \frac{1}{2}\rho_g A_d C_D |u_{rel}| \tag{2.24}$$

Where C_D is the drag coefficient which is a function of the droplet Reynolds number Re_d and the cross-sectional area of the particle A_d.
According to Schiller and Naumann [16], the drag coefficient of a single sphere is given as follows:

$$C_D = \begin{cases} \frac{24}{Re_d C_p}(1 + 0.15 Re_d^{0.687}) & Re_d < 10^3 \\ 0.44/C_p & Re_d \geq 10^3, \end{cases} \tag{2.25}$$

The particle Reynolds number with the domain fluid viscosity μ_g is,

$$Re_d = \frac{\rho_g |u_{rel}| D_d}{\mu_g} \tag{2.26}$$

The Cunningham correction factor dependent on Knudsen number Kn is given as follows,

$$C_p = 1 + Kn_p(2.492 + 0.84 e^{\frac{-1.74}{Kn_p}}) \qquad \text{with } Kn = \frac{\lambda}{D_d} \tag{2.27}$$


The mean free path length λ in gaseous phase can be computed as,

$$\lambda = \frac{k_b T_g}{\sqrt{2}\pi d_g^2 p_g} \tag{2.28}$$

Where mean molecular diameter in gas phase $d_g = 2 \times 8^{-10}$ m.
The force F_{ig} adds the effects of gravity and buoyancy,

$$F_{ig} = V_p \cdot (\rho_p - \rho_g) g_i \tag{2.29}$$

F_{ip} is the pressure force of the incoming droplet, given as,

$$F_{ip} = -V_p \cdot \nabla p \tag{2.30}$$

F_{ivm} is the virtual mass force bringing into account acceleration/deceleration of the medium surrounding the drops, particles or bubbles. This is treated by increased inertia of the Lagrangian parcels (half mass of displaced fluid is added). The additional force term finally reads as follows,

$$\overrightarrow{F}_a = -\frac{1}{2} m_f \left(\frac{d\overrightarrow{v}}{dt} - \frac{D\overrightarrow{u}}{Dt} \right) \tag{2.31}$$

Where m_f denotes mass of displaced fluid, $\overrightarrow{v}$ is the parcel velocity and $\overrightarrow{u}$ represents ambient flow velocity.
The other forces like the virtual mass force, the magnetic or electrostatic forces, the Magnus force etc. are encapsulated by F_{ib}.

The atomization process of sprays is then accounted for with distinctive submodels , present in FIRE™, one of which is discussed in the section to follow. The droplets post this atomization, are kept tracked of in a Lagrangian way through a grid used for solving gas phase partial differential equations, simultaneously taking into account, the coupling of gas and liquid phases.
The limitation of DMM [15] is that the Lagrangian parcels are treated as point sources for mass, momentum and enthalpy in the frame of the Eulerian gas flow field. An improvement for this method is currently under way for AVL FIRE™ based on [17].

2.3.2.1.2 SCR Evaporation submodel with Thermolysis

Out of the many sub models available, one relevant to Thermolyis equation, related to the Evaporation of Ammonia discussed in section 2.2.1.1 is briefly explained.

The injected droplet is heated up in the hot exhaust gas stream. At high temperatures the evaporation of the liquid starts.As water's boiling point is less than that of Urea's, the vapor which evaporates first consists mainly of water. Whether also urea vapor is produced is questionable, since urea is known to decompose directly via thermolysis in section 2.2 from solid or liquid phase. Thus in the FIRE approach, following the PhD thesis of Birkhold [6], a two step process is modeled.

- Pure water evaporation until the drop consists of only Urea.
- Urea decomposition leading to subsequent NH_3 and HCNO formation.

The evaporation rate for the thermolyis is given according to [6] as,

$$\frac{\mathrm{d}m_{urea}}{\mathrm{d}t} = -\pi A D_d \cdot exp\left(\frac{-E_a}{RT}\right) \tag{2.32}$$

where A is a constant in kg/ms, E_a is the activation energy in J/mol, D_d is the droplet diameter, R is the Universal gas constant in J/Kg.K and T as Temperature.

2.3.2.1.3 Kuhnke/Wruck Wall Interaction and Wall Heat Transfer Subodels

This is an advanced wall interaction model, and takes into consideration T_w or wall temperature besides the splashing parameter K defined as follows

Depending on a dimensionless wall temperature

$$T^* = \frac{T_w}{T_s} \tag{2.33}$$

ad a dimensionless droplet velocity of

$$K = \frac{(\rho_d d_d)^{3/4} u_{d,\perp}^{5/4}}{\sigma_d^{1/2} \mu_d^{1/4}} \tag{2.34}$$

with,
T_w as the wall temperature, T_s as spray temperature, $u_{d,\perp}$ is the droplet velocity orthogonally incident on the surface, suffix d is for droplet while σ is a standard deviation of Gaussian distribution defined as,

$$\sigma = \sqrt{\frac{2}{3}k} \tag{2.35}$$

with k being turbulent kinetic energy.

The Kuhnke [18] model solves for four different regimes indicated with the figure 4 as follows.

- **Deposition**: If the wall temperature is less than 1.1, and droplet velocity is low then the impacting droplet are completely deposed on the wall and create a wall film.
- **Splash**: If the wall temperature is higher than 1.1 along with higher impact velocity, the particles are atomized and smaller droplets are formed. A fraction of the droplet mass is then transferred to the wall film.
- **Rebound**: At higher wall temperatures and a low impact velocity, a vapor layer between droplet and wall is formed. This sheet prevents a direct contact of the droplet with the wall, leading to a reflection of the impacting droplets. At this high wall temperature no wall film temperature occurs.

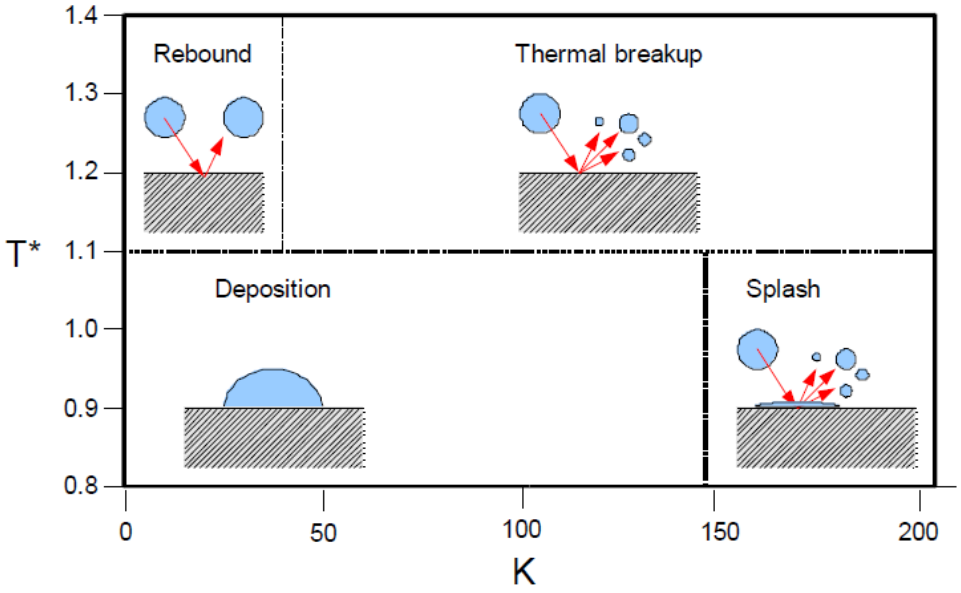

Figure 4: Regime map for Spray wall interaction according to Kuhnke[18]

- **Thermal breakup** At higher wall temperatures ($T^* > 1.1$) and higher impact velocity, the droplet also disintegrates into secondary drops. Here also no wall film is formed.

2.3.2.2 Wallfilm module

A brief idea about the wall film model[19] is shown. There are first some assumptions to consider which help form a better understanding.

- This is two separate single phase models attached at the film surface instead of a two phase model. This is done by modifying boundary conditions.
- Film thickness is very small compared to mean diameter of the gas flow, making volume grid unnecessary.
- The wavy surface of the film is not simulated in detail but modeled by a mean film thickness with superimposed film roughness
- The mean film surface is assumed to be parallel to solid wall.
- The above assumption lead to an implementation of the wall film model as 2D finite volume method on the wall boundaries of air flow geometry.
- Die to thin film and its small velocity, wall friction and the inter facial shear stress dominate the film behaviour as compared to inertial forces and lateral shear.
- Wall temperature is below Leidenfrost point.


As the film thickness is large, erroneous results can occur due to the neglect of inertial and curvature effects

The basic governing equation for the wall film flow is the film thickness equation[19]. For simplicity, a Cartesian formulation is presented here.

$$\frac{\partial \delta}{\partial t} + \frac{\partial \delta u_1}{\partial x_1} + \frac{\partial \delta u_2}{\partial x_2} = \frac{1}{\rho A}(S_{mD} - S_{mV}) \tag{2.36}$$

Now, instead of solving for the velocity components u_1 and u_2, convective terms

$$\frac{\partial \delta u_1}{\partial x_1}, \frac{\partial \delta u_2}{\partial x_2} \tag{2.37}$$

can be evaluated, and equation 2.36 can be explicitly solved, assuming that the velocity components are known, along with the Source terms S_n.

Therefore, primary interest is the method of determining the film velocity components, obtained with various film velocity profiles.

2.3.2.2.1 Film Velocity Profiles

The forces acting upon the film result in shear forces which the film exerts to the wall. This distribution of shear forces relates to the velocity profiles. The Velocity profile of film due to applied shear forces τ is given by,

$$\frac{\tau}{\rho} = (\nu + \epsilon_m)\frac{\partial u}{\partial y}. \tag{2.38}$$

2.3.2.3 Thin walls module

This module[20] was used to model solid wall boundaries as

- As thin, walls, that can be solved for transient heat conduction, in the normal direction
- As thin walls, where the 1D heat equation is solved in both lateral and normal direction.

This includes solving the following equation within the thin wall definition

$$\frac{\partial T}{\partial t} - \frac{\lambda}{\rho c_p}\frac{\partial^2 T}{\partial x^2} = 0 \tag{2.39}$$

with t as time, x as coordinate in direction perpendicular to wall, T as temperature λ as thermal conductivity, ρ as density and c_p as constant of specific heat.

2.4 Optimization with HEEDS

The aim of this thesis is to study optimization and find trends as well as insights on the design spaces that will and could provide an optimal solution. In that endeavour, quite a few capabilities in terms of various optimization types, response surface methods, post processing insights, etc, are explored within the state of the art software of HEEDS-MDO from the perspective of Scania and especially NXPS where EAS are at the central focus.

2.4.1 Basic Terminologies

There are quite a few Optimization related terms [21] that will be used and have been also used so far a few times. A brief clarification is provided

- **Optimization**: The process of finding the best design, or the optimal design from all the possible designs that can be generated from a set of parameters can be briefly termed as Optimization. For instance, a pipe required to produce minimum pressure drop for a given length, is allowed to have some constraints on its radius, as this can be changed to find which configuration would give the best pressure drop, finding such a design then becomes an Optimization problem. In short, process of making something as fully perfect or effective as possible, with potential constraints, is known as Optimization.

- **Parameters** The variables (input variables, design variables, project variables, independent variables, input function etc), that can be changed to obtain a new configuration with a combination of its defined range are called as parameter. For instance, In the current study, various dimensional parameters within the CAD model of the model under scrutiny are defined as parameters. The space formed with n parameters will be

$$x_1, x_2, x_3....x_n \tag{2.40}$$

  where each of these parameters will have a range, so e.g. x_1 could be length having a minimum and maximum value as limits, and so on.

- **Design** Each such different configurations obtained by changing the parameters are known as Designs. (This is represented by the dots on the plot with Design IDs on x-axis in figure 17).

- **Response** The variables (dependent variable, output variable, output function, etc) that are to be observed as a result of changing these parameters. For instance, in the current study, surface uniformity, and pressure drop are defined to be a responses of the study.

- **Baseline**: The optimization study (function) in HEEDS requires a base design in order to rank its results, this is done by comparing it with the parameters and response values of a baseline design.

- **Objective function**: An objective function is a response that has been chosen by the experimenter as a a value which represents a physical quantity, to be minimized or maximised. For instance, if a design is outlined to have minimum time to market, then time becomes the objective function which should be minimized. Similarly there can be multiple objective functions like the one in current study, where the pressure drop is to be minimized, surface uniformity is to be maximized and wall film mass is to be minimized.

- **Competing Objectives**: Improving one objective makes the other objective worse, then these objectives are said to be competing. e.g. minimizing time for a production may require maximizing resource investment for it. This type of objectives are sometimes known from previous experiences and sometimes not.

- **Performance**: HEEDS gives each design a performance rating. The value returned for an objective(s) and the degree to which a constraint is satisfied, if any, determines a design's performance value. A high performance design satisfies all constraints and has good rating on its objective (s). It is a single number calculated from all responses.

  Normalizing is then done onto a response value. This is because for e.g. two objective functions such as Pressure drop, has the order of 10^5 Pa while the other objective function of surface uniformity is always between 0 and 1. To obtain a single performance number, both of these response values are normalized with the baseline values, as follows,

$$\frac{\text{[pressure drop]}}{\text{[baseline model pressure drop]}} + \frac{\text{[surface uniformity]}}{\text{[baseline model surface uniformity]}} \tag{2.41}$$

  The performance number (function) can now be calculated as

$$P = \sum_{i=1}^{N_{obj}} \left(\frac{LinWt_i * S_i * Obj_i}{Norm_i} + \frac{QuadWt_i * S_i * Obj_i^2}{Norm_i^2} \right) - \sum_{j=1}^{N_{cons}} \left(\frac{LinWt_j * ConstVio_j}{Norm_j} + \frac{QuadWt_j * ConstVio_j^2}{Norm_j^2} \right) \tag{2.42}$$

  where,
  N_{obj} is the number of objective functions defined in the study, $LinWt_i$ is the Linear weight for ith objective, default = 1, S_i is the sign assigned for objective functions, -1 if to be minimized and +1 if to be maximized, Obj_i is the response value for the ith objective for that design, $Norm_i$ is the normalizing value for the ith objective from 2.41, $QuadWt_i$ is the quadratic weight for the ith objective, default is set to 0, N_{cons} is the number of constraints in an optimization study, (zero for current study), $LinWt_j$ is the Linear weight

for ith constraint, default=0, S_i is the sign for objective function, -1 if it is to be minimized and +1 if it is to be maximized, $ConstVio_j$ is the amount by which jth constraint is violated, set to 0.0 if the constraint is met. $Norm_j$ is the normalizing value for the jth constraint, $QuadWt_j$ is the Quadratic weight for the jth constraint, default = 0,

- **Dominance** Design A is dominating against Design B if it is better in at least one objective and no worse in all other objectives.

  e.g. if both objectives are to be minimized, 3 scenarios are possible

  - A dominates B
  - B dominates A
  - A and B are non dominated

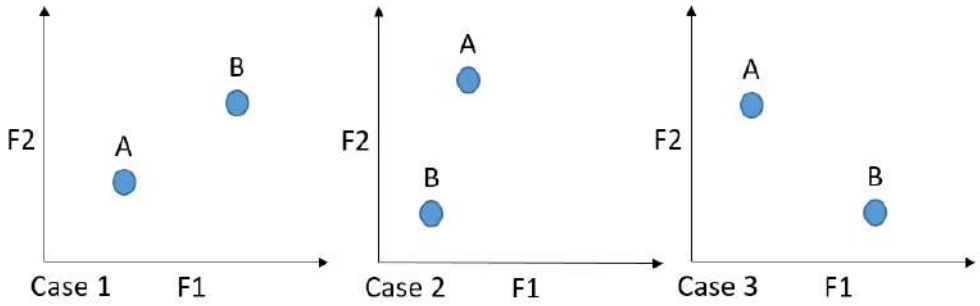

Figure 5: 3 Possibilities between Design A and B with both objectives to be minimized

- **Pareto front** During the run, feasible designs that are not currently dominated by any other designs are given the first rank. The remaining designs are re-ranked and those that are not dominated by any other design in that group are given the second rank. The procedure is repeated, until all the designs in the set are ranked. The set of designs that are not dominated by any other designs found till now is called the Pareto set. The set of designs that are not dominated by any designs in the entire search space is known as the Pareto front shown in figure 6. As the run progresses, the Pareto sets continue to approach the Pareto front (the set of ideal solutions) [21]. If there are multiple ranks, then size of a bubble is also used to indicate the rank. Bigger the bubble, higher the rank, less dominant the design.

- **Latin Hypercube Sampling**: LHS is a sampling technique where each variable to be sampled is divided with with equal probability into number of requested segments(n). These segments, depending on the probability distribution selected, (Normal distribution will have larger segments closer to the mean, and Uniform distribution will have equal segments). This essentially

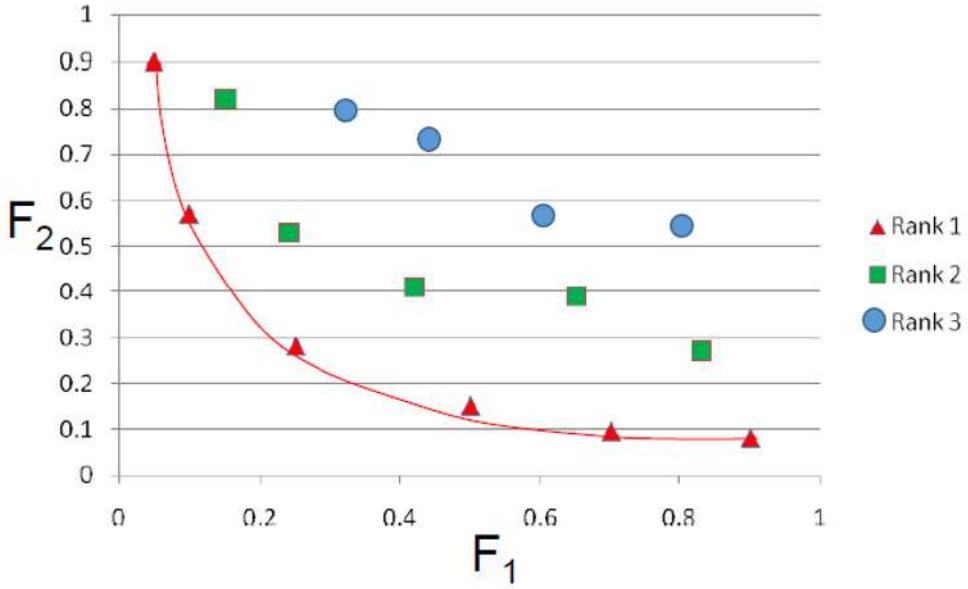

Figure 6: 3 Ranks, along with the best ranks indicating a pareto front

forms a sampling space that each row and column in a particular hypercube of partitions has exactly one sample, making the sampling space, evenly spread out, and not randomly.[22]

- **Surrogate** : See section 2.4.4, (used interchangeability with meta model, approximated model, response surface model, etc). It is essentially and approximation built from the observed sampling of the data.

- **Cross Validation**: Cross Validation and its residuals are used to judge the predictive powers of the approximated model and in identifying outliers, if any. (Outliers will be the entities that reduce the accuracy of the surrogate). They tell how well a surrogate predicts the values for the unknown designs, not evaluated in the generation of the surrogate.
  This is done by setting aside some known designs, fitting the remaining designs with the surrogate and then using the removed data to test with the reduced surrogate.

  This is done by partitioning a random combination of designs in question into k subsets of almost equal size (this is known as K-fold Cross Validation). One of these subset becomes the test set, while $K-1$ sets become the train sets. For each removed design, HEEDS uses the model to estimate the response at the test set and compare it with the train sets. The difference is the cross validation residual. The values shown in the tables from the results section are the RMS values of the Cross Validation residuals.

  This means that a good value of cross validation residual is relative to the absolute value of the given response and its range. It also varies according to the problem at hand. The scatter plot for Cross Validation Residuals is hence


plotted against the approximated objective response to better understand the accuracy of the fit.

Ideally the residuals, just like any residuals, should be as near to zero as possible. If that is the case, the 3D response surface will be a very good approximation of the original function. However, if the residuals dots are not all densely nearby the line indicating zero, this indicates the relative error in the approximation that can be expected. The extent of which, will be decided by the % value obtained in HEEDS. This is recommended to be below 5% by HEEDS, although care should be taken. Also, if one or two designs which are separate from the majority of the designs in the scatter plot, even if the scatter plot values are very near to zero, then such designs could be later found as outliers appearing with pointed peaks and dips in the 3D response curve. This is a sure indication that the design was an outlier, and it must be removed from the data set, in order to use only non outlier designs to form the approximation. The plot also should be devoid of any patterns (increasing, decreasing curves etc) and should be mostly flat or symmetrically distributed around zero.

A recommended method from HEEDS is to deduce and interpret a cross validated value after conducting several K fold cross validations within HEEDS. If the there is a significant variation in the cross validation number after each iteration, the fitting surface will be ill represented.

Sometimes, a good approximation, and hence a good cross validated residual values are also not obtained because of the lack of the original sampling data. This is indicated with a $R^2 < 1$ values. As the approximation is built on the originally existing space, it is recommended that the higher sampling will lead to a better approximation fit. However, this also increases the chances of finding more outliers to deal with.

- **Shape Factor**: The shape factor in HEEDS controls the amount by which each data point affects the approximated surface. Small shape factors extend each point's influence, while large shape factors contract each point's influence. Smaller shape factors tend to give a rounder shape between points, while larger shape factors tend to let the surface fall away to the underlying polynomial.

- **Design of Experiments**: A DoE, essentially helps find a yes or no answer for a parameter, if it is the one that will affect a response or not. It aims to obtain as much information regarding the trends from a parameter space as possible with as minimum sampling points as possible. So a degree to which this parameter is affecting the response, can also be understood. This then helps screen out such parameters from the design space. It is usually a common practice to run a DoE study first to obtain a brief understanding of the design space, and then an Optimization study in that refined design space.

2.4.2 Weighted Sum Parameter Optimization

Here, a Sum of all objectives defined in the study, yields one total objective. From P in section 2.42, the weighting factors are used to assign relative importance to the objectives. e.g. consider two objectives F_1 and F_2 with no constraints, the simplified version of section 2.42

$$P = W_1 * F_1 + W_2 * F_2 \tag{2.43}$$

hence, for a given value of weight factors W_1 and W_2 we get one optimal solution, while changing the ratio of W_1/W_2 , we get different optimal solution.

The way this works in HEEDS is it uses multiple search methods in a blended manner, which are a combination of global and local search methods. Each participating approach contains tuning parameters that automatically gets updated during the course of the search. All of which is done with the SHERPA [23] algorithm of HEEDS.

2.4.3 Multi Objective Parameter Optimization

It[21] is used when there are multiple objectives in the study, as well as when they are of competing nature. in such a situation there is no single solution that is optimal. This works like Weighted sum objective, but it can handle objectives independently to provide a set of solutions. It seeks to find the trade-offs among multiple objectives. This gives a surface of design points, all of which are optimal, known as Pareto front. A design must then be selected considering the trade offs.

SHERPA[23], here sets optimal designs dominating over others. A design is said to dominating when, it is better in at least one but not worse in all other objectives. During the run, feasible designs that are not currently dominated by any other designs are given the first rank. The remaining designs are re-ranked and those that are not dominated by any other design in that group are given the second rank. This is repeated for all the designs. The set of designs that are not dominated by any other designs found till now is called the Pareto set. The set of designs that are not dominated by any designs in the entire search space is known as the Pareto front. As the run progresses, the Pareto sets continue to approach the Pareto front (the set of ideal solutions).

2.4.4 Response Surface Methods

RSM (meta modelling) are mathematical techniques useful for improving or developing insights on an optimization processes. This is extensively used in industrial applications where there are several or at least some potential influencing variables onto the performance measure or quality characteristic of the output [24]. The automotive sector being one of them. These methods, as claimed in [25], helps with the decision making process for design engineers.

In HEEDS[21], the response surface method uses linear, quadratic, or other functions (in terms of the variables) to approximate the response. A significant

advantage of using response surfaces is that the actual defined objective function, which might be very time consuming to compute, is not evaluated in searching for better points on the response surface, potentially saving a lot of time. It should also be noted that because these are approximated models, there is no guarantee that the minimum or maximum value obtained from the response surface will exactly correspond to the actual objective function. Some error is to be expected. Consider a response y that depends on parameters x_1, $x_2...x_k$ as [24]

$$y = f(x_1, x_2.., x_k) + \varepsilon \tag{2.44}$$

with ε being sources of variability unaccounted in f and it is treated as a statistical error having a normal distribution with mean zero and σ^2 variance.

Because the true response function is unknown, f needs to be approximated[24], which is done with **Kriging** Meta model in the current study, and a Gaussian tuning process.

Essentially, Kriging is a class of methods coming from field of geo-statistics [26], providing a prediction, linearly depending on the original sample space such that the weights depend on the kriging model or the design, but not on the observations. The tuning process for this kind of mapping is given as follows:

The Gaussian process is a widely used tool in spatial statistics as well as computer experiments because of its desirable properties. This is simply because of it's unbiased estimation for training samples and error estimation for the unknown sample[27]. As explained in [28], it forms,

$$g(x_i) = \beta^{\mathrm{t}} f(x_i) + \varepsilon(x_i), i = 1, ...n. \tag{2.45}$$

with f_x as predefined functions and β as set of unknown coefficients. Here ε is realization of Gaussian process with

$$cov[\epsilon(x_i), \epsilon(x_j)] = \sigma^2 R(x_i, x_j) \tag{2.46}$$

$$E[\varepsilon(x_i)] = 0 \tag{2.47}$$

This is a function of distance between x_i and x_j measured in Euclidean space by assigning weights as

$$d(x_i, x_k) = \sum_{h=1}^{d} \theta_h \left| x_{ih} - x_{jh} \right|^{p_h} \tag{2.48}$$

with θ_i and p_i are scaling and power parameters, Gaussian correlation is when $p_h = 2$, and h= 1.

The first term of equation 2.45 is mostly modelled with a lower regression model, as having a higher degree polynomial function over fits the data [29].

Note that the value of θ_h affects the smoothness and prediction capacity of the Kriging model. Small values smooths the prediction while, at large values, Kriging model has accurate predictions near sampled points, but false predictions elsewhere.

Compared to other meta models techniques, the biggest advantage of Kriging is that the model gives an error estimation between predicted and truth value, as

$$MSE = \sigma^2 \left[1 - r^T R^{-1} r + \frac{(1 - f^T R^{-1} f)^2}{f^T R^{-1} f} \right] \tag{2.49}$$

$$\hat{s} = \sqrt{MSE} \tag{2.50}$$

where σ^2 is the variance, r is the correlation vector between the new point to be predicted and the training sample. R is the mutual correlation matrix of the training samples[27].

To conclude, various terms and fundamentals have been set to interpret the current study. We now use the tools, which help us build this study.

Chapter 3

Method

This chapter outlines the method to setup this study. This includes integrating 5 softwares that were used. Please note, due to the confidential nature of the work, much of the setup details will be hidden, although an elaborate version of setup to this method has been submitted to Scania CV as an internal report for it's knowledge base archives. Broad strokes pertaining to the setup are given.

3.1 General Setup

The general setup is to discuss the settings and other related setup that is required before using the 5 softwares. As Scania operates over a huge network across multiple simulation teams, each Engineer is allocated different resources for his/her work.

For this current study, a 12 cores Windows 10, Enterprise as well as a 12 cores Red Hat Linux version 6.10 desktop systems were available for this Master thesis. There were two separate systems used because the softwares used on the OS was restricted with the available licenses at Scania. So we see a division of following softwares as per their OS, commonly practiced at Scania.

- CATIA V5 — Windows only
- ANSA — Linux only
- HEEDS — Both, but majorly used in windows
- STAR-CCM+ — Both, but majorly Linux
- AVL-FIRE™ — Linux only

3.1.1 Windows and Linux connection

The first course of action was to set the communication between both the available OS's. This was done by setting up a read and write access to a directory over the file system. Note that, two desktop systems are most of the times not available to every simulation engineer, as most work with solely windows or solely Linux

environments. Although remote profile could also be set, if there is no other OS available.

This was done by setting up a Putty connection between the local node, from where HEEDS is run, and the Linux system that will use other Linux based softwares. HEEDS provides an instruction to set this up.

3.1.2 Resources settings

Now as the CFD simulations employed in this study are resource intensive. For STAR-CCM+, this was for a 2M mesh cell size explained in section 1.4, So a 100 step iteration took roughly under 5 minutes per design, depending on availability of 350 cores selected to run this study. However, for AVL-FIRE™, this simulation time for 6M cell size took 2 hours on average per design. For STAR-CCM+ , two resources were used for conducting these simulations

- Pooling in local linux based system and connecting them to form a localized cluster
- Scania's HPC cluster where all the simulation teams run their studies.

These two were used as per the traffic on the cluster, or according to the availability of other Linux systems to the author. Although most of the times, clusters were used, especially for studies related to AVL-FIRE™.

3.1.3 HEEDS Settings

Once, the network access, read write access, as well as cluster settings are done, HEEDS, requires this putty connection to be readable to it. This is done by providing the public and private key pair of putty explicitly to HEEDS in the directories across both OS's which will be used by HEEDS to conduct it's study.

Similarly, HEEDS should be able to access this cluster, to submit it's studies directly. This is done by setting up remote profiles in HEEDS which are actually Cluster specific details. For the current study a IBM based LSF job scheduler was employed.

3.1.4 Softwares

As there were 5 major softwares used for this study (one being HEEDS itself), a broad stroke on their settings is provided.

3.1.4.1 CATIA V5

CATIA V5 is employed as a CAD tool to model, various EAS geometries according to the design direction that is being explored by Scania's engineers.

As each sampled design will open CATIA during each new evaluation, it is important, that the CATIA module remains available, when it's license is requested.

Other wise, there will be either a certain time penalty, according to the environment variables set for it, or the evaluation might not proceed with HEEDS, resulting in a failed evaluation of the design.

3.1.4.2 ANSA

ANSA is a meshing software, which is state of the art for commercial industrial applications. This tool was used to obtain the surface mesh of the CAD model, after defining the geometry according to the study in the CAD model with CATIA. The setup only requires a CFD setting, as there are other options available too in ANSA. It should be noted that the current study is configured in ANSA to be used in batch mode.

3.1.4.3 STAR-CCM+

STAR-CCM+ being the state of the art simulation software used for CFD within NXPS at Scania. This is solely because of the capabilities it's mesher and solver provides to simulate and obtain understanding of complex phenomena. It is also very user friendly and the automation capabilities with java programming language are theoretically limitless. The post processing capabilities of STAR-CCM+ also make it an ideal software for Scania for it's internal development reports.

3.1.4.4 AVL-FIRE™

This Linux only based tool, is used to model spray simulations as well as combustion simulations for which it's solver provides better capabilities compared to STAR-CCM+. This tool is also required to run in batch mode, and is set accordingly with various options. There are various supporting applications within the AVL-FIRE™ catalogue which were also used in the current study to either test the setup, scripts or debug the workflow for the current study.

- FIRE_C™, or FIRE classic is the AVL's version of a simulation environment. All the pre-processing and post processing definitions are defined in this software.
- FAME_M™, is the poly meshing software that uses surface and edge meshes to generate a volume mesh.

There are various files that are to be obtained as a post processing results, but, the current example limited its use only generating 2D plots for various entities under observation.

3.1.4.5 HEEDS

There are quite a few settings to keep in mind when working with HEEDS, but the major ones are for each of the portals defined in the following section are as follows

- **Finish Condition**: When a study is underway, (think software running its study), HEEDS will continue to do so, unless a condition is defined that explicitly commands its to stop and move forward. This condition is termed as finish condition, which marks the end of the software usage for a design under scrutiny. This could be a dummy file, or a parameter value, or an if condition for a parameter value and many more such possibilities. In the current work, it is mostly a file that is printed out to mark the end of the process. and hence a flag given as in form of finish condition.
- **Success Condition**: After a software usage is over, HEEDS should know, if the aim of the study done by the software usage was achieved or not. This is defined with the help of Success condition. This generally can be a again a separate dummy file, or a keyword that is looked for from the files that is already generated, or even a check in terms of until a file is produced and so on.

3.2 STARCCM+ with HEEDS

For the present work, for Optimization of CFD with HEEDS, the following setup was established. This is broadly explained as follows.

Figure 7: STAR-CCM+ setup with HEEDS

Each square seen above represents a software that is used for a particular. These are known as portals. When a portal is not with brown background, it means the software is accessed or run on the remote machine which is a Linux environment in the current study. (Portals, 2, 3, 4 are Linux based). The other two portals represent a local installation of the software, hence that particular software file will be readable in that environment. The small icon seen on the top right corner of portals 2, 3 and 4 are Linux environment and cluster environments logos respectively. (i.e Portal 2, is run on linux machine, while 3 and 4 are run on the cluster). All the five softwares mentioned in section 3.1.4 are used in this setup.

3.2.1 Methodology

Once the HEEDS settings are set, each portal is set one by one to perform and set it's steps necessary for the succeeding portal, in the following manner,


- **Catia_1**: The CAD model is imported, and all the parameters are tagged onto it, with HEEDS. These were length radius and angle definitions for the current study. The parameters were then given a ranges. Defining a distribution for this range is also possible but, this was not done in the current study. The portal ran for $\approx 20s$ per design.

  This also forms the starting point of the current study. The dimensions tagged in this portal are already tested before so that, the upper and lower bounds of these parameters are either known, or are set as constraints by the designers. This forms the basis of numerous designs that will be generated by changing and sampling the combination of parameters. The finish and success condition are taken as default in this portal.

- **Ansa_Mesh_2**: Once the CAD model is set with parameters, and a range is given to all of them, this portal, then was used to obtain the surface mesh of the CAD in form of a STL file. This was achieved by a python script, which makes sure there are no unmeshed surfaces or conflicting surfaces for the subsequent steps. The portal ran for under $\approx 50s$ per design.

  The finish and success conditions are defined accordingly, keeping in mind STL file with all the defined named selections, is the absolute output that is required out of this portal.

- **Star_mesh_3**: In this step STAR-CCM+ is used to import the above mentioned STL file and perform a surface meshing operation. This surface meshing is different from the one done in step 2 because, the STL file is now updated to a STAR-CCM+ file, with all the named selections defined previously intact. Using 16 cores, this took an average of $\approx$ 11 minutes per design.

  The finish condition and success condition depends according to the problem being conducted, although, in the current setup a file prompt after the cluster run is complete, is requested.

- **Star_run_4**: Once the surface meshing is done, a java macro, along with this STAR-CCM+ surface mesh file is submitted onto the cluster for volume meshing as well as running the simulation in one step itself. (Meshing is done in two steps at Scania because of the clusters configurations for the same, however it is possible to do in one step). On 350 cores, this took $\approx$ 1 minute to run 100 iterations per design.

  The finish and success condition , here are the files and reports that must be generated after the cluster completes the simulation correctly. This is manually set at Scania's environment.

- **STAR_CCM_5** This is the final post processing step, where all the results obtained after running the simulation on the cluster is accessed for images, plots, reports, etc. All of these are previously defined in the STAR-CCM+ file that submitted or is made to print out with a help of a java macro. Retrieval took $\approx$ 2 minutes per design.

Essentially, one design theoretically should complete in an average 15 minutes, however this was seldom the case, due to the resources available on the cluster, and even license conflicts within Scania from other users of the same software.

A **Design evaluation** is now defined to be the sum of all of these 5 steps for the duration until number of evaluations to be conducted is reached. (In the 3 studies conducted with STAR-CCM+, this number is 50, 200 and 250, as will be seen in the sections to follow.) A **feasible** design will be the design which achieved it's success condition for all the portals in the study and finally, producing a result which the study was defined. A **error** design will be the one which did not succeed in the success condition, and hence stopped the evaluation.

3.3 AVL FIRE™ with HEEDS

With AVL FIRE™ the setup follows a similar workflow, however, as the files that are generated with AVL FIRE™ are different than the ones produced in STAR-CCM+, its, input and output files for each portals become specific to the AVL Software used. Another change that can be observed here, is the thumbnail images that has been added in the first and the last portal to showcase that particular design which is currently being evaluated.

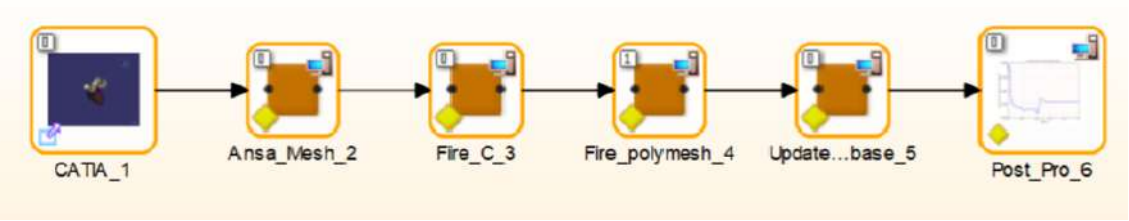

Figure 8: AVL FIRE™ setup with HEEDS

3.3.1 Methodology

For AVL FIRE™ , the following steps are set,

- **Catia_1**: The CAD model is imported, and all the parameters are tagged just as in section 3.2.1. A range is defined on each parameter.

  This becomes the starting point of the current study where numerous designs are generated one by one by changing and sampling the combination of parameters, which is done by HEEDS itself. The finish and success condition are taken as default in this portal. The portal ran for $\approx 46\ s$ per design.

- **Ansa_Mesh_2**: Once the CAD model is set with parameters, and a range is given to all of them, this portal, was then used to obtain the surface mesh of the CAD in form of a STL file with the help of a python script just as step 2 of section 3.2.1. The finish and success conditions also remain the same.


- **Fire_C_3**: In this FIRE_Classic is used to first import the STL file from the previous step and generate a surface as well as edge mesh files as are required by AVL volume meshing software in the next steps.

  Hence these files are given as finish and success conditions. The portal ran for a little over 1 m per design.

- **Fire_polymesh_4**: Once the surface and edge meshes are generated from a previous step, this portal, generates the volume mesh after importing the previous surface meshes into itself.

  Hence the volume mesh file then becomes the finish and success condition for it. The portal ran for a little under 4 m per design.

- **Update_base_5**: Is the portal where, this volume mesh updates onto an already defined sample case, which has all the solver settings and plots definitions. Then this newly updated mesh is assigned the solver settings, after which it is submitted to the cluster for simulation.

  The success and finish condition, are the cluster output files and the keywords defined in those files. As this is the step where simulation is done, the average run time per design was 1H:50 minutes.

- **Post_Pro_6** For the current study only 2D plots were defined to be obtained, although a 3D post processing result is also possible to define. The resulting portal, runs a python script to plot a .dat files of 2 columns that is defined in the volume mesh file, before it is submitted onto the cluster.

  Here the finish and success condition are these images, that are obtained after the .dat files are run with the python script to plot and save the data as png files. This took 20s per designs

Essentially all the steps completed in $\approx$ 2 hours per design, for a 6M mesh cell size using 192 cores on cluster and 12 cores for local portal runs.

To conclude, a method to set an optimization study with HEEDS has been touched upon due to the confidential nature of the work. All five softwares have been introduced and their contribution towards a generating the result for the current study has been shown.

Chapter 4

Results and Discussion

The results section is majorly divided into 2 categories as there were different objective functions observed for flow and spray CFD simulations. Optimization results for both of them are discussed

Internal flow simulation is conducted with STARCCM+. It gives an understanding about parameters affecting the mixing as well as uniformity of the flow at a section in the evaporation unit (section 2.2). Three different studies are discussed in this category

- Design of Experiments / Screening Response on 50 Design Evaluations.
- Multi Objective Parameter Optimization on 200 Design Evaluations.
- Weighted Sum Parameter Optimization on 250 Design Evaluations.

For this flow simulations the objective functions will be

- Pressure drop (Minimize)
- Surface Uniformity (Maximize)

Note that objective function is not required for a DoE study, hence the above two objectives are valid for only first two studies of 200 and 250 Design evaluations.

For Spray simulations conducted with AVL FIRE, the following objective functions are studied

- Pressure Drop (Minimize)
- Surface Uniformity (Maximize)
- Total Wallfilm mass (Minimize)

This study shows the design space for 3 objectives against one another, ranked over with the third objective function.

A comparison between the best result from the DoE and two optimization methods is discussed indicating an expected trend of higher the number of evaluations, better design found.

4.1 Flow analysis with STAR-CCM+

4.1.1 Design of Experiments/Screening Response

For Flow simulations, in this section, focus is kept on a parameter oriented study. This is to understand with a simple study, using only one objective function of maximizing surface uniformity as discussed in section 2.3.1.2. The study is conducted on 50 designs chosen with 6 parameters, as explained in section 2.4.1. The DoE aims to gain insights to the design space with minimum experiments, an arbitrary method available within HEEDS to select number of experiments were chosen along with Latin Hypercube Sampling (refer section 2.4.1) method. The following section discusses the qualitative and quantitative affect of parameters on this response of surface uniformity. And talks about the approximated model developed from this space of 50 evaluations.

First, A correlation plot is studied to find the parameters that affect surface uniformity the most. This is also done to screen out the other parameters that do not affect the surface uniformity indicated with SU_023. Designs, are visually observed to obtain the best performing design. Note, as this is a DoE Study, it does not require an objective function and there is no constraint on maximizing or minimizing the response to be set manually, but in this case, a design which yields maximum surface uniformity is to be looked at manually.

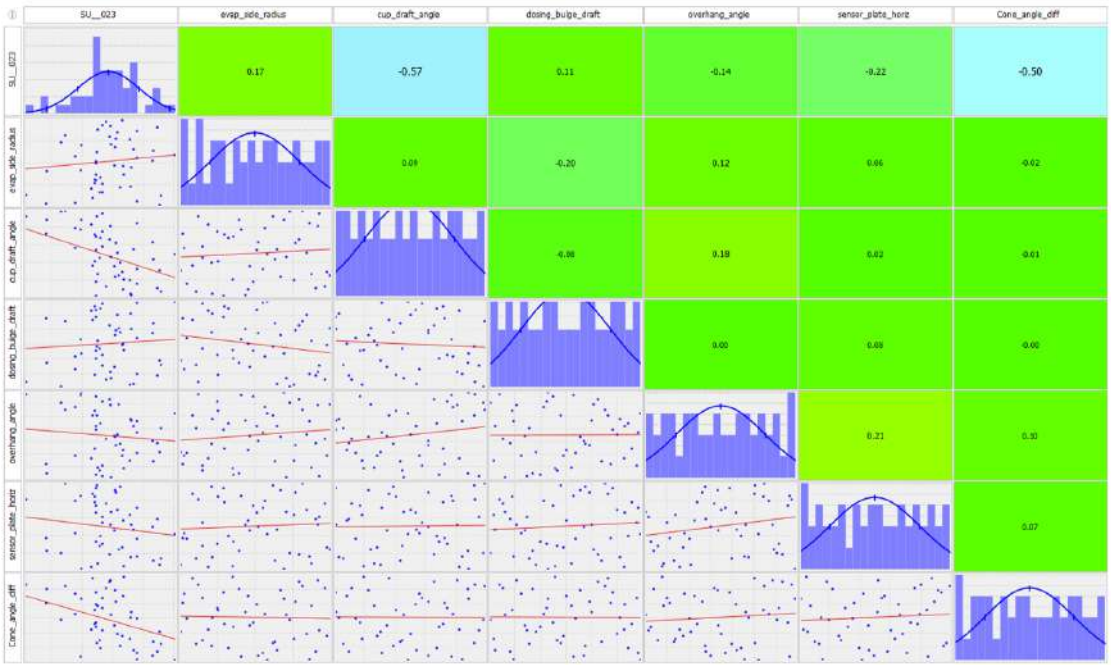

Figure 9: Correlation between all involved parameters with the response

In figure 9, all the parameters observed in green and sky blue are the ones affecting surface uniformity (plotted onto x-axis of each cell of the first column, while parameters are plotted on y-axis of the each changing row). So for instance,


Cell(2,4) will have the column name as x-axis and a row name as y-axis. As for now, only the response is studied, so the x-axis under observation will be the 1st column which is of SU_023.

It can be observed from the figure 9 that the correlation between the parameters can also be obtained if the column chosen is other than the first. In this case, we do not find any such high or low correlation between any two parameters. This is expected since it is a Design of Experiments, the sampling of the parameters should not lead to any correlations.

The blue dots present in the lower triangle of the correlation matrix, not including the first column, indicate the goodness of Latin Hypercube sampling for the parameters for the design space. It is then in the first column of response function, where this sampling is observed in regards to the parameters that are supposed to affect it.

This is indicated by the number shown in the upper triangle of the matrix, along with the colors indicating a quantitative measure for the same. The number essentially becomes the slope of the trend line shown in red.

The diagonal elements indicate this distribution for a parameter (as both x and y-axis will be of the same entity). This distribution is not to be confused with a normal distribution, even if the graph appears to be so.

Note that the trend line corroborates with the sampling space shown by the blue dots. If this is not the case, or the trend line is not indicating the direction in which the sampling dots are observed, then this usually means, that more evaluations should be conducted. However, this does not seems to be the case here.

The parameters that are affecting the surface uniformity the most are those seen in sky blue color. This is also evident with the high negative slope of lines observed in 1st column of this plot. Negative value, as well as the slope shown by the trend lines simply means, increasing the parameter will lead to the loss of response value.

Having understood the design space with 50 evaluations for 6 parameters, an attempt to build an approximated model (meta model, response surface, surrogate model) from this now existing design space is made.

4.1.1.1 Response Surface for DoE Study

A response surface is developed keeping these two parameters in mind. Namely Cone angle difference and cup draft angle for a response of surface uniformity (obtained from previous correlation plot). This is done because the original evaluation of 50 designs took roughly 14 hours to complete. (Sometimes subjective to the computational resources available at Scania, due to the number of Engineers accessing the same, simultaneously). Although 14 hours is not high, this model is to speed up the design evaluation process even more.

This response surface aims to see how closely it can fit the original design space, in order to conduct other optimization/DoE/Experimental studies that would have been conducted on the original design space, but this time only in fraction of minutes. Another valuable insight is the validation of completely new designs that are obtained with the Kriging model, with the original design space of 50 evaluations.

The response surface is developed with a Kriging model, having a Gaussian function as explained in section 2.4.4 and with equation 2.45 as defined in the following table.

Type	Function	Tuning	Shape	R2	RSME	CrossV
Kriging	Gaussian	Fast Kriging	0.331645	1	0	0.00166

Table 1: Modelling settings for DoE Study

As explained in section 2.45, the model offers error estimation capabilities, which are observed with RSME and R2 values which are the classic least square methods, while the shape factor, (refer section 2.4.1) fine tunes the this Kriging model.
As explained in cross validation of section 2.4.1, the value of 0.00166 can still be a relative one, and hence, after running few iterations to obtain this value, following table is observed, and then the surrogate response function residual (y-axis of figure 10 is plotted with actual surrogate response value itself on x-axis). The cross validated values are shown in

Cross V		
SU_023	Value	Difference(%)
Actual min	0.90233	0.184
Actual mean	0.907735	0.183
Actual max	0.912096	0.182

Table 2: The mean value of the surrogate response, obtained from the training and test sets as defined in section 2.4.1

The plot for cross validated residuals plotted against response is shown in figure 10. This is done to study the accuracy of the fit for the surrogate.

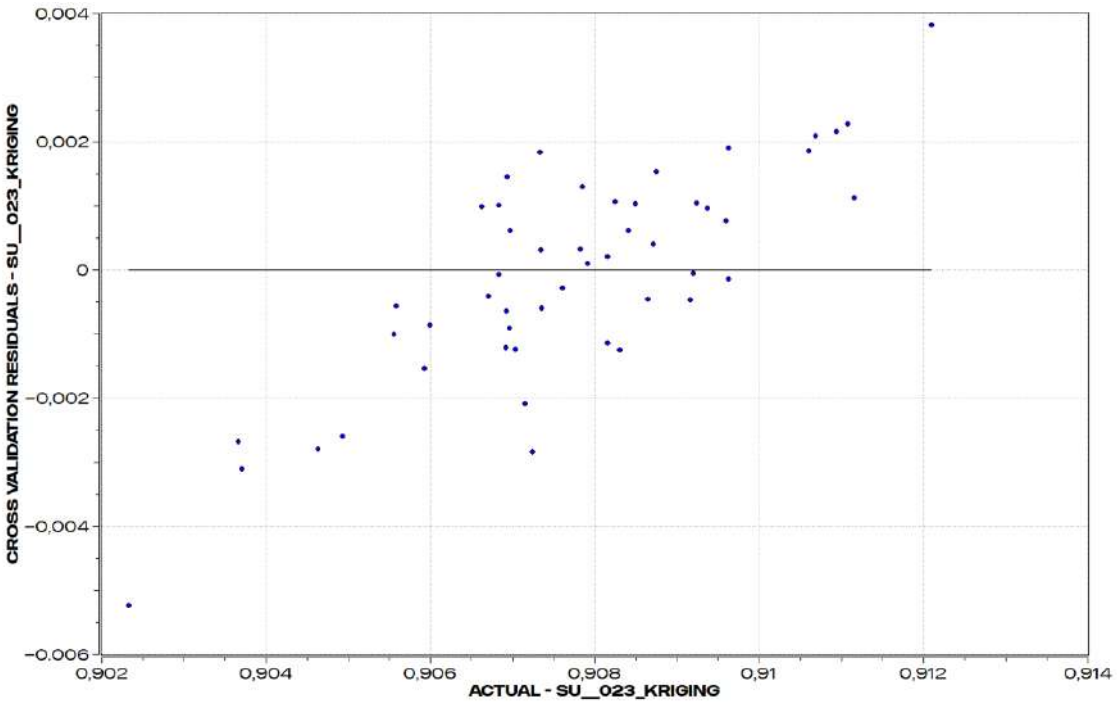

Figure 10: Cross validation of Kriging response of SU_023 residual plotted against Kriging response of SU_023

This plot shows that their residuals are mostly very close to zero as discussed in cross validation of section 2.4.1. This indicates that the major designs out of 50 lies in between ±0.002, in terms of their residuals. As well as no single design is far away from the majority of designs, so an outlier is not expected here. However, this graph should ideally be symmetrical to the zero axis. This is also not the case here, which means there are still some improvements that could be done.These improvements are not performed here in order to build a quick approximation to find improvement for the design space hence all the original designs were chosen.

Note that, most of the designs should either lie on the zero line or should be symmetrically spread, for goodness of the fit, but, in this case, the residuals still stay under the margin indicated by the table 2.

(The y-axis is named as such to define the modelling function used for the study, as HEEDS has many modelling functions available to choose from, this name convention helps to keep track of the many plots generated.)

4.1.1.2 Surrogate for DoE Study

Having obtained a fairly decent cross validated residual value, along with no indication of an outlier design, within the figure 10, the surrogate model is now build and run, within minutes, to obtain a modelled design space for response of surface uniformity.

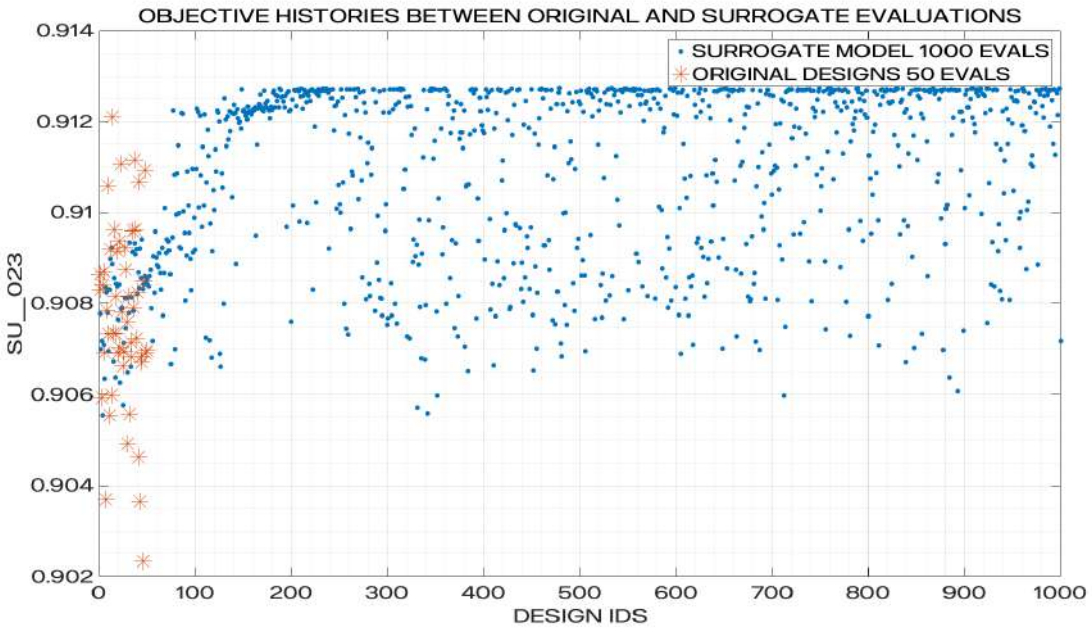

Figure 11: Objective history of surrogate plotted with original 50 evaluations.

Figure 11 clearly indicates that the response surface has found a slightly improved region than the originally evaluated design space. This is seen by the blue dots which are above the topmost orange dot for the y-axis. It is also indicates, with the current setup, the maximum surface uniformity, the system is capable of reaching. Another important conclusion to draw is that in order to reach the best design, at least 190 or 200 original evaluations would be required before the optimal value is for best surface uniformity is obtained. However, the response surrogate gives this idea, within 50 evaluations only. This does not improve any further.

Now, as we know from figure 9, two parameters affect the surface uniformity the most, these two parameters are now evaluated for a surrogate.

Figure 12 shows a comparison between the 1000 evaluation for the parameter of cupdraft angle done against the surface uniformity response. This indicates a small margin of improvement which is still possible from the existing design space of 50 evaluations. The best design with the original evaluation reached a Surface uniformity of 0.91209, while with the 1000 evaluations approximation, the best suggested value is 0.9127. This is a slight increase. Furthermore, an important insight on the parameter value is obtained that keeping parameter value between 25 and 26 degrees will yield the optimal surface uniformity. This is hardly evident from the 50 evaluation design space in orange. Hence, the current surrogate was able to give an direction to achieve this optimal design.

Similarly, for the other parameter of Cone angle difference, the newly obtained design space from the surrogate is shown in figure 13, which indicates a margin of improvement to maximize surface uniformity. It also indicates the value that should be kept in order to achieve this optimal response.

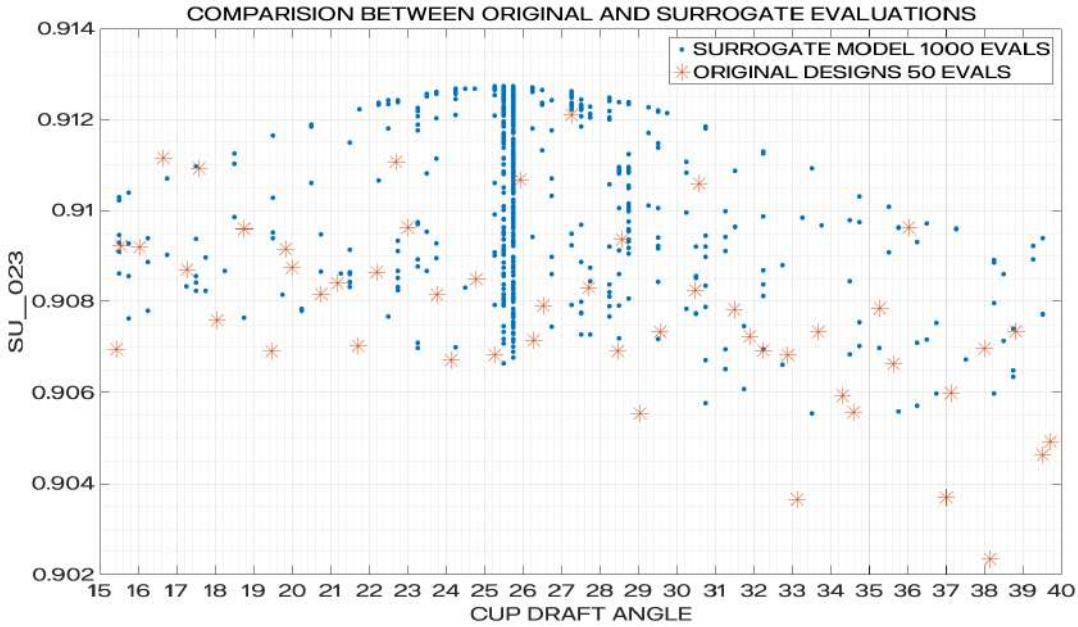

Figure 12: Objective history for RSM cupdraft angle with original 50 evaluations.

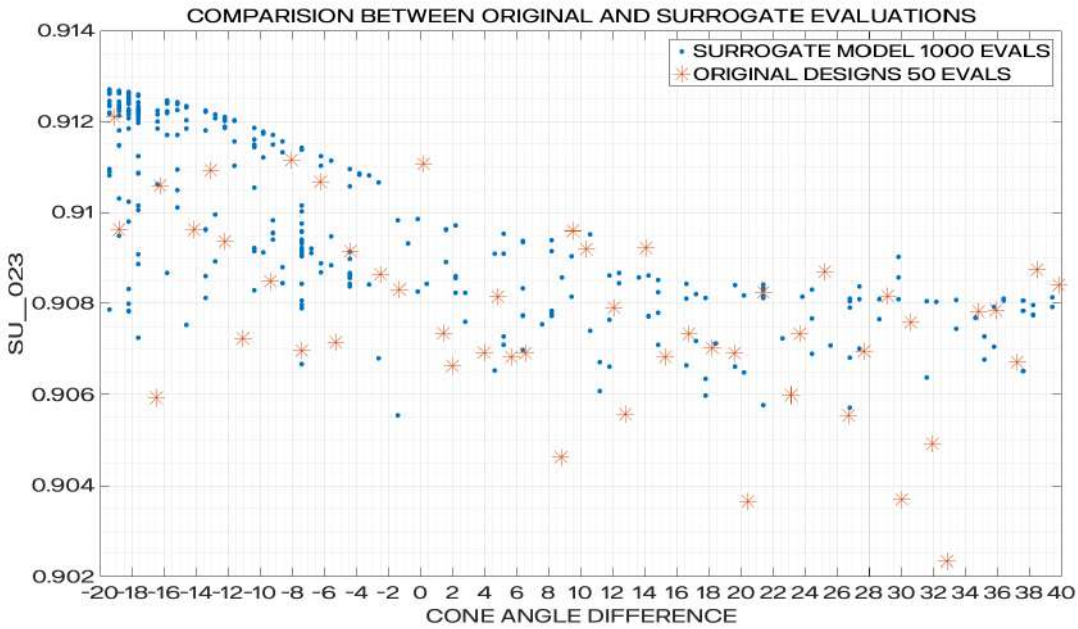

Figure 13: Objective history for RSM cone angle difference obtained with original 50 evaluations.

The combining response surface is plotted to build a coherent understanding of the two parameters affecting surface uniformity.

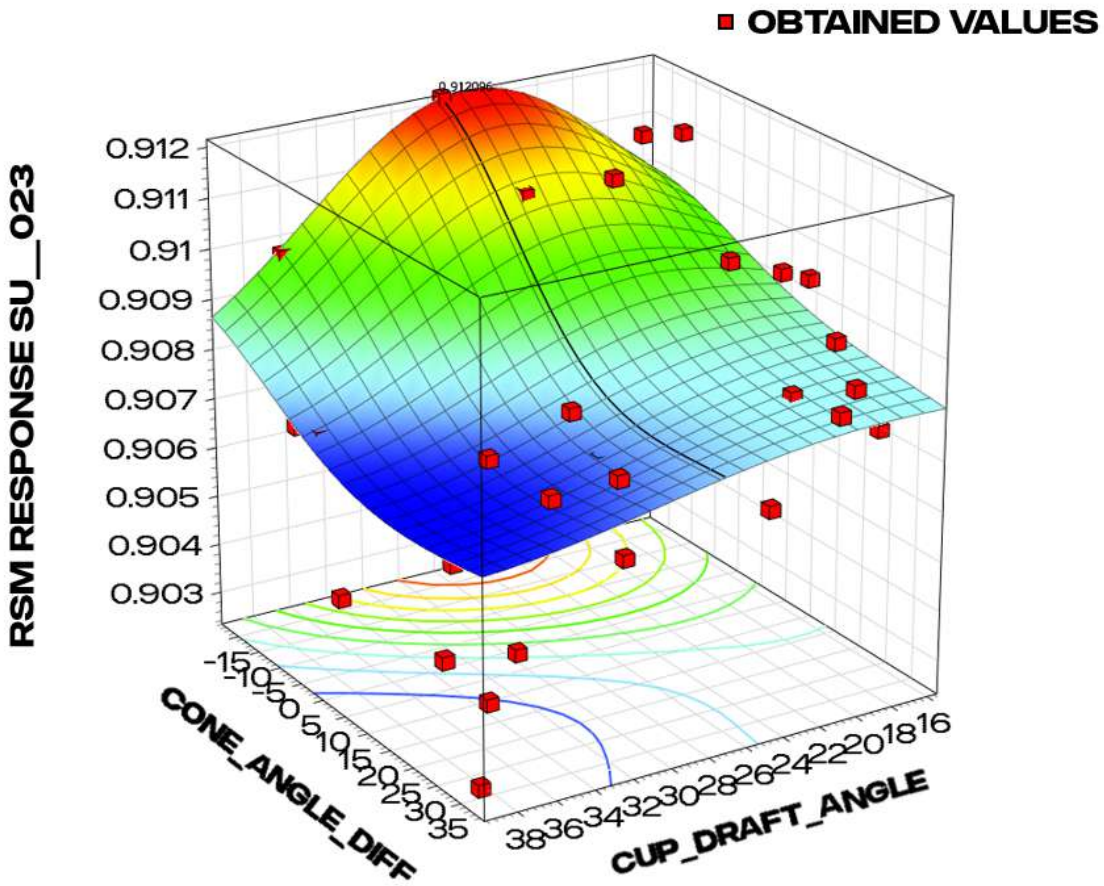

Figure 14: 3D response curve for 2 parameters for Kriging response of SU_023.

figure 14 indicates the response surface for both the parameters combined at the best design of the evaluated space. The red dots represent the original 50 design evaluation space. Note that some points will be hiding directly behind the curve shown above.

It can be concluded that creating a simple DoE study with one objective response of surface uniformity gave an indication for a scope of improvement however small (0.07%). But it showed the fact that an optimal design would have been found after 190th evaluation, which was deduced from the sampling of 50.

4.1.2 Multi Objective Parameter Optimization

Having understood the design space with a Design of experiments, the complexity is now increased by adding another objective function of Pressure drop to the study. Another parameter was also added to slightly scale the base model from the previous study.

A multi objective parameter optimization explained in section2.4.3 is now conducted with 200 design evaluations and the 2 objective functions of minimizing pressure drop and maximizing surface uniformity. This is done in order to understand the design space that will help minimize the pressure drop and maximize surface uniformity simultaneously. (Hence the name multi objective). An insight to the results in the following design space reveals the competing behaviour between the two objective functions. The necessity of a trade off between the two, for an optimal design is apparent. Top 30 designs are then ranked in Figure 15 and as clarified in section 2.4.1.

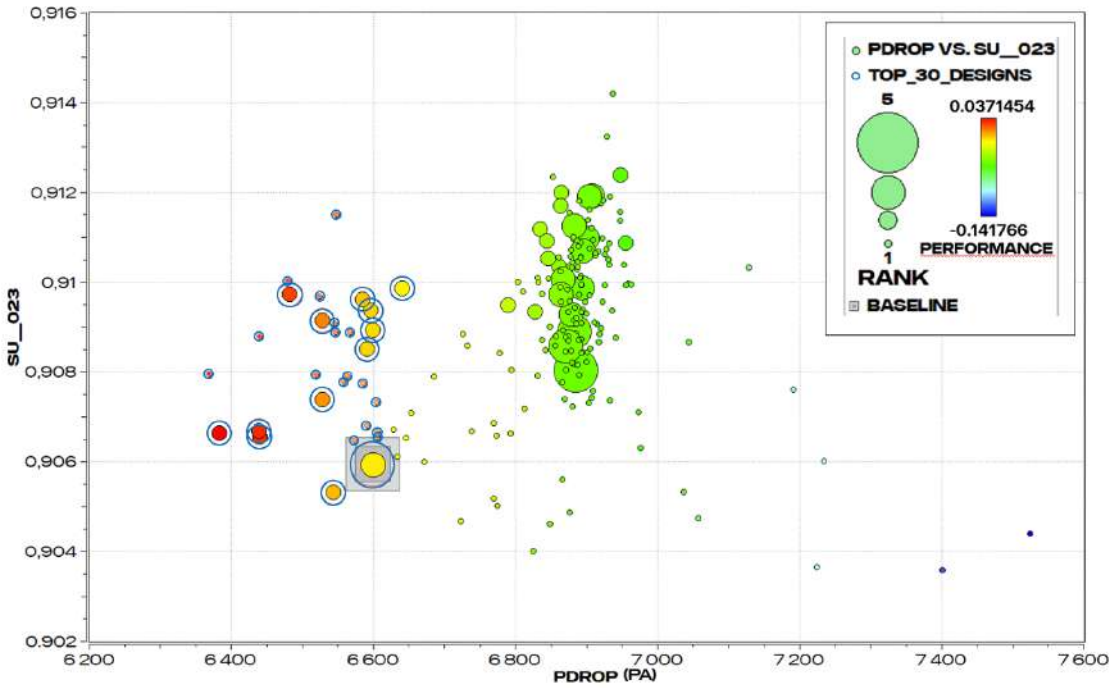

Figure 15: Pareto Plot showing design trade offs between pressure drop and surface uniformity

Figure 15 is presented on 4 dimensions. i.e. the two axis representing the objective function, and a rank and performance.(see Performance, Pareto Front, and dominance of section 2.4.1). Here Pressure drop is defined to be minimized and Surface uniformity is defined to be maximized. (SU_23 is a Scania's naming convention, where the section under observed must be identified with the part it is present on. The number 23 signifies this offset distance on the part.). A smaller rank(tiniest dots) indicates a better design, but it should also be according to the performance legend. As HEEDS has a relative measure of this rank in between


any of its two designs (refer figure 5), the higher the performance the better value this design gets in finding its place on the plot. So if a design has best pressure drop (global minimum), best Surface uniformity (global maximum), is ranked best compared to other design (figure 6), and has a good performance number, it will be represented by the tiniest dot in red signifying best of all 4 dimensions. This can be seen in the smallest dot just before 6400 Pa, which is the obtained best design evaluation among the 200 evaluations. Top 30 such designs are highlighted in blue concentric circles.

Note that the the tiniest dots (good rank) in the higher pressure region, has a low performance number, so, they become bad design. Even if they were to form a pareto front design for more number of evaluations, the designs at both ends of the pareto front are to be ignored. Hence the smallest dots in high pressure region will be ignored, if they are still in the pareto front. In the same way, green colored tiniest dots in the 6800 Pa to 7000 Pa region, have moderate performance number, hence, they are ranked good as they still are good in one objective function of surface uniformity (refer figure 6). In a similar fashion, the bigger bubbles in green are ranked low, because relatively, they are neither good in both objectives (figure 6), while having a moderate performance number. It is clearly observed that a slight offset in any one of the objective direction in this case, has led to a drastic change in the rank of the design, hence the difference in size is observed, even if few of those designs are in the same vicinity.

The Top 30 designs that are indicated with concentric circles, are just the subset of the original 200 evaluations, and are shown to indicate their relative presence on the plot.

It can be seen that in order to have minimum pressure drop with maximum uniformity, the designs should ideally be in the top left corner of the plot. But, there are no such designs in that region, indicating, the competing behaviour of the two objective functions. This gives an insight as well as quantitative data to the designer, whether a design with better pressure drop or better surface uniformity should be chosen for further investigation. A decision needs to be made regarding the designs with trade off between both or any number of objectives. This plot helps with the Quantitative values associated with each are available to compare the relative difference between any two designs from the figure 16. A baseline design is shown in the grey square so as to be a reference for other designs, as is the requirement of any optimization study.

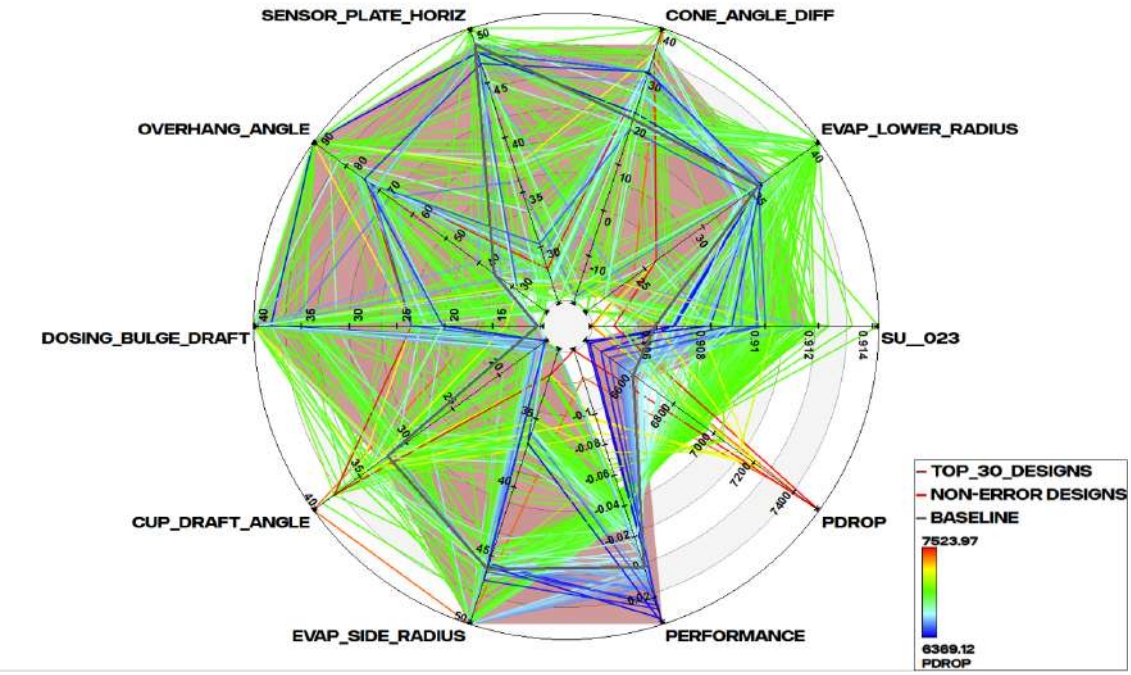

Figure 16: Radial plot for non error and top 30 designs

Figure 16 shows each of the parameters range between a maximum and a minimum value with minimum values towards the center. Essentially, a polygon will contain all the parameters necessary for a design, with its corresponding response values. The colored lines indicate all the non error designs in order of their pressure drops (Non error designs are the designs that did not crash due to conflicting/overlapping parameters, or simply due to a failed mesh). Few blue lines in the inner region indicate the relatively better pressure drop designs. The region marked in red form the design space of these top 30 designs available for exploration.

The parameters that were defined are now seen here, whose combination forms the design space, there were 7 compared to previously defined 6 in the DoE study. The other two are the objective functions of pressure drop in Pa and Surface uniformity. The performance number has also been added as a starting point to pick the design, in case, the pivot is one of the two objective function.

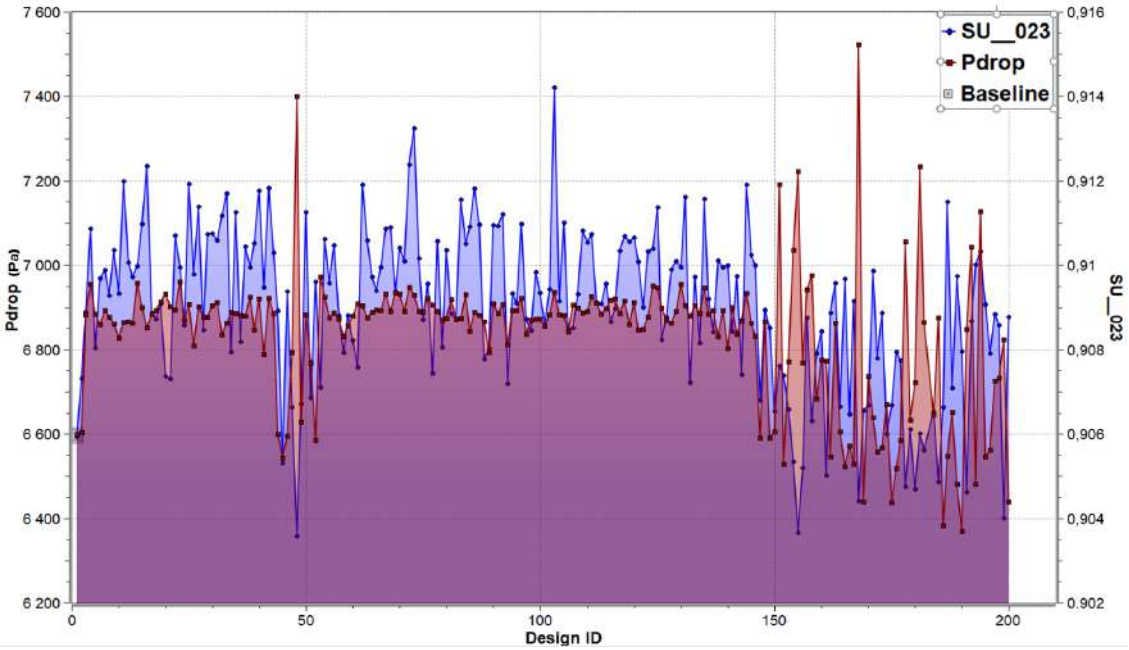

Figure 17: Surface uniformity plotted with Pressure drop to observe the variation between the two objective function value distribution.

Figure 17 shows the design IDs plotted against pressure drop and Surface Uniformity. This is to indicates that the best pressure drop performance was obtained at 190^{th} evaluation shown by bottom most point in red. While the best Surface uniformity design was obtained at around 100th evaluation (topmost point in blue). Hence it is inconclusive from the number of evaluations conducted regarding how soon the most optimal design would be found, from the perspective of the delivery times for a development project. The baseline design is seen at the very start of the objective history.

4.1.2.1 Response surface for Multi Objective Study

From the previous study of DoE, it was found that a a slight improvement was possible. An objective function is now added along with a new parameter to increase the complexity of the model. A similar method is then solved with the aim to find a better design space than the original evaluations. Now as figure 15 did not have any designs in the upper left corner of the plot, which was satisfying both the objective function, an approximated model is developed to see if such a design space could be found or not.

The response surface is developed with a linear Kriging model, having a Gaussian function as explained in section 2.4.4 and with equation 2.45,

Response	Type	Function	Tuning	Shape	R2	RSME	Cross V
SU_023	Kriging	Linear	Gaussian Process	7.50673	1	5.43e-6	0.00185
Pdrop	Kriging	Linear	Gaussian Process	0.412384	0.826	66.5	130

Table 3: Response approximation values for Multi objective study

In this table we find the R2 error for the Pressure drop response to be less than 1. We also observe the RSME to be not zero unlike the DoE study This usually means two things [21].

- The data chosen for the sample is noisy
- More number of evaluations needs to be conducted.

But after running a few iterations for the various models and functions available in HEEDS, the minimum difference as shown in table 4, was obtained with the Kriging function and a Gaussian process.

Cross V		
SU_023	Value	Difference(%)
Actual min	0.903587	0.207
Actual mean	0.909041	0.205
Actual max	0.914216	0.204

Cross V		
Pdrop(Pa)	Value	Difference(%)
Actual min	6369.12	2.05
Actual mean	6836.08	1.91
Actual max	7523.97	1.73

Table 4: Cross Validation values compared for both objective functions for Multi objective study

The two response values are then checked with the Cross V residuals against the obtained values of the same response as follows.

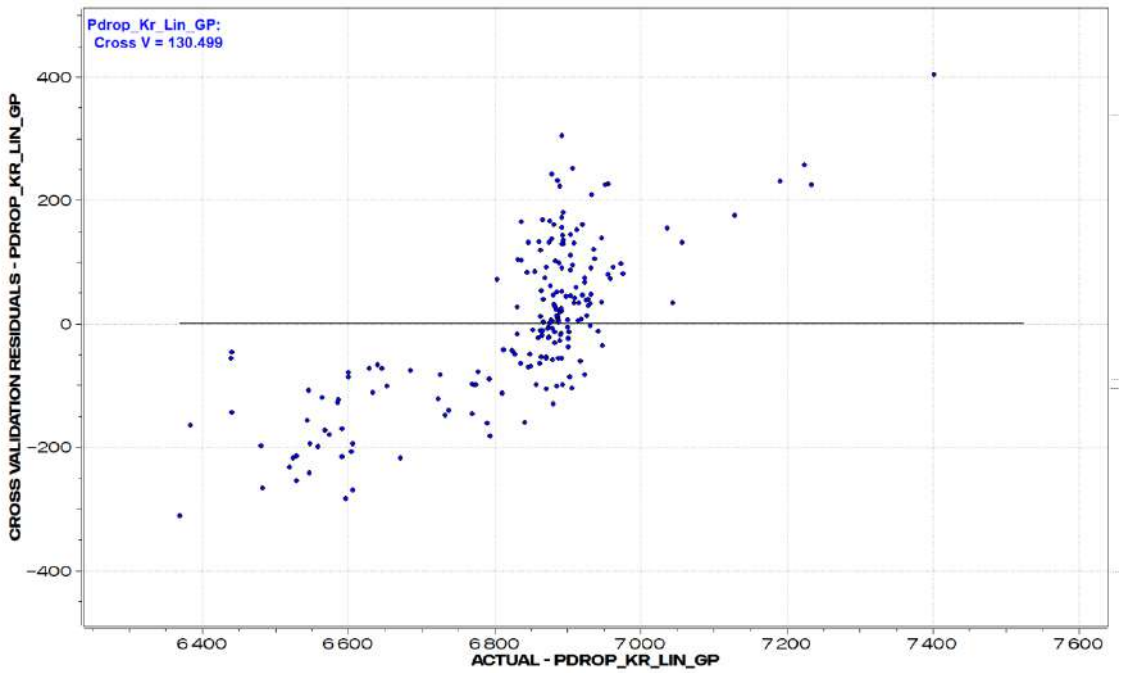

Figure 18: Cross V residuals plotted against obtained Pressure drop values

We again see a trend in figure 18 shows a few designs away from the trend although they are still not far enough from majority of designs to be termed as

outliers. Although it is possible to obtain an outlier point in the surface plot. The cross residual value of 130 obtained for pressure drop, seems to still lie under the 5 % value as recommended by HEEDS, and hence this modelling settigs were chosen. Note that these is using a sampling for all 200 evaluations without any seclusion, hence, there is a scope of improvement by reducing or selecting the number of designs used to built this response surface.

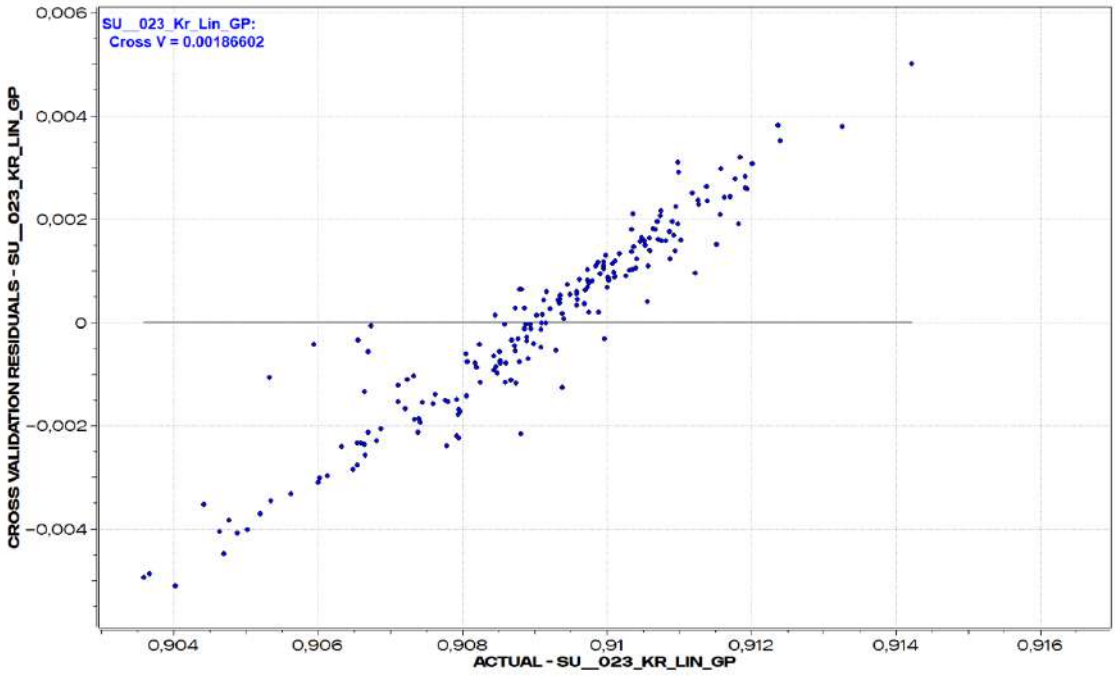

Figure 19: Cross V residuals plotted against obtained Surface Uniformity drop values

figure 19, behaves almost similarly to figure 10, but the sampling is more. We see few of these going above the ± 0.002 limits, and hence indicating that the error shall be more compared to what was observed in the DoE study.

4.1.2.2 Surrogate for Multi Objective Study

The cross validated values does not give much confidence for Pressure drop (figure 18) response, but show similar behaviour for the Surface uniformity response (figure 19) from the previous study. So it is expected that the design space, obtained from this model, will indicate this fact.

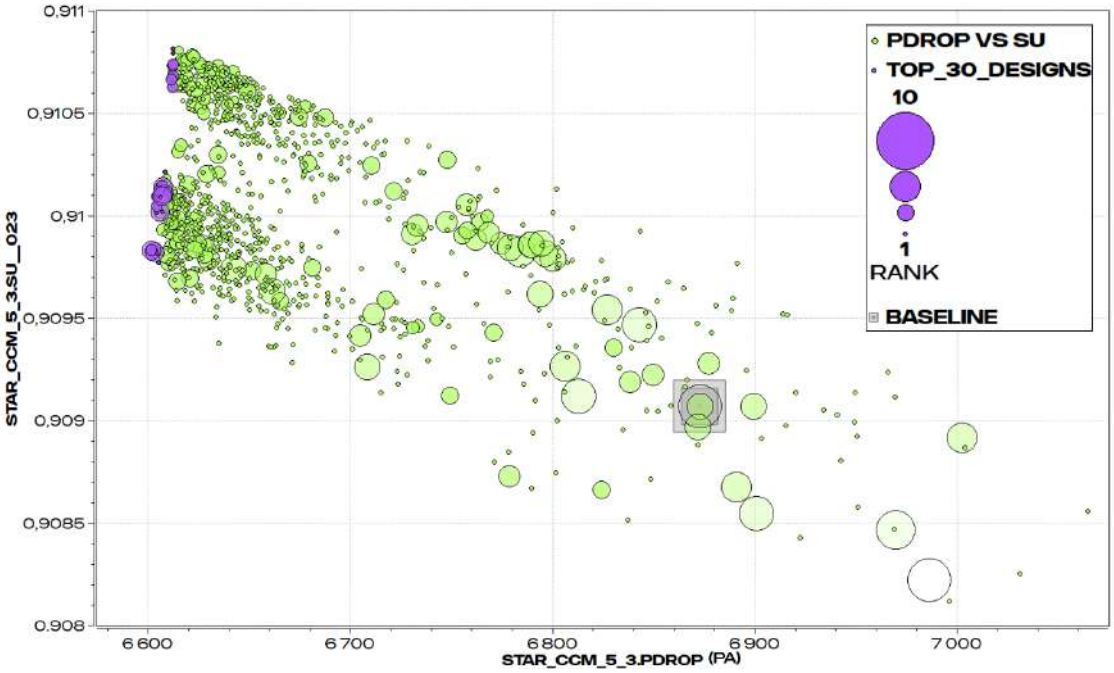

Figure 20: Response surface pressure drop and surface uniformity, indicated with rank of designs

Figure 20 shown the region of the 1000 evaluation space, to be where it is required, i.e. with minimum pressure drop and maximum surface uniformity, however, a closer look in figure 22 shows a much clearer picture of this design space.

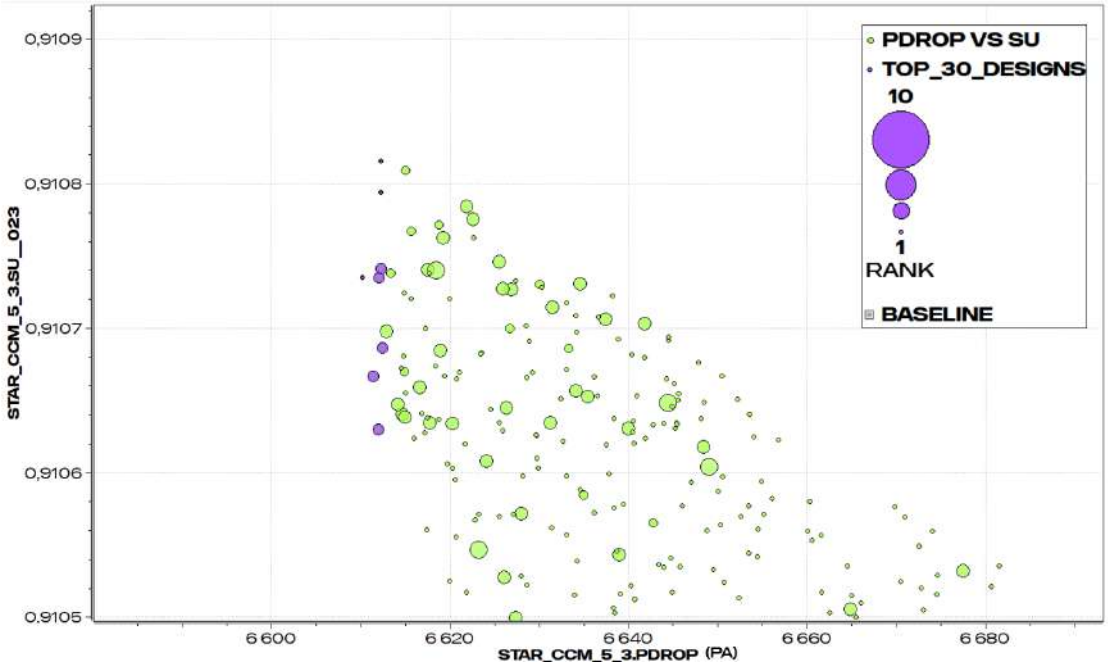

Figure 21: An inset to the optimal region of figure 20

Figure 20 gives the result where it is required, i.e. in the upper left hand corner which has the maximum surface uniformity and minimum pressure drop. Top 30 designs are shown in purple.

(Note, the axis names were not changeable, due to HEEDS settings. As HEEDS uses its own naming convention to keep the track of parameters and variables coming from different study (or softwares). This is set as such because, if names could be changed then, the parameters and hence the design space could also be changed. However, surrogate models are only relevant if the design space is not changed).

Now, to get the comparison between the original evaluated design space and the proposed surrogate, figure 15 is plotted on figure 20 as follows.

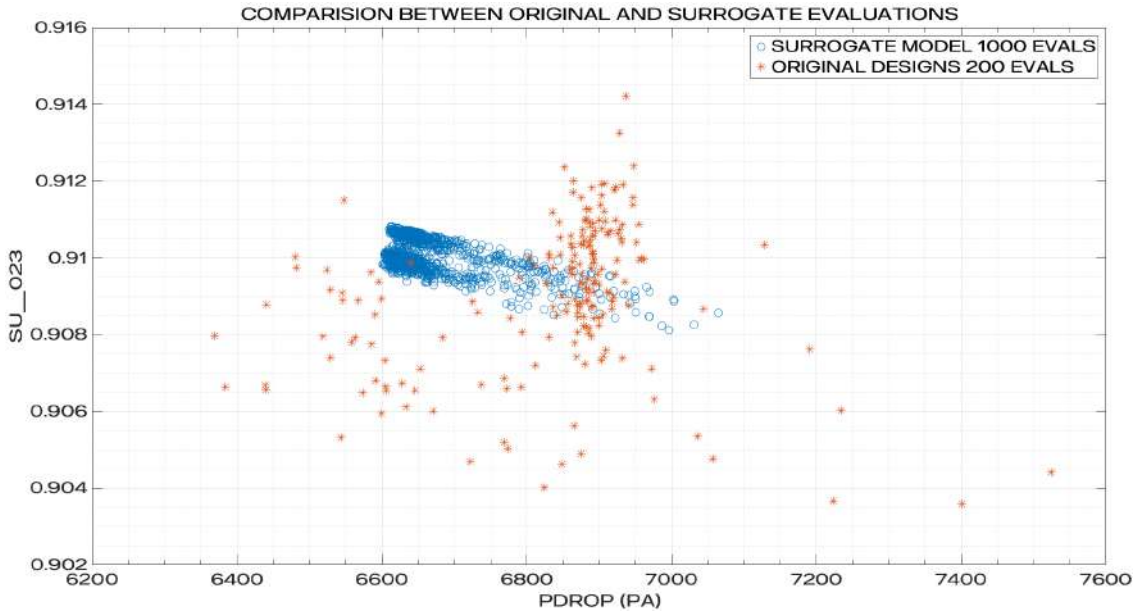

Figure 22: Comparison between Surrogate and Original model

Figure 22 shows original evaluations (orange crosses) that ran for the complete simulations for 200 designs giving some idea where the optimal designs should exist.($\approx$ 6550 Pa). Blue colored circles are 1000 evaluations from the approximated model. It can be clearly seen that the percentage difference of $\approx$ 2% observed for pressure drop and marginal difference observed for surface uniformity in Table 4 can be seen between the orange and the blue design spaces. Hence the approximated model, in this study does not indicate any region for better performance than the original sampling. However, the error remains in a very close proximity, along with a completely new region for exploration.

It should be noted that the region marked with blue is obtained with very less computational power or time investment. Hence a completely new design space was achieved within matter of minutes with the surrogate but not with better design than the original 200 evaluation indicated. Even more important fact is that the design space in blue is better than majority of the original 200 evaluated space both in terms of Pressure drop as well as Uniformity.

To conclude we find that the relative ranks of the 200 designs evaluations, while with a rough surrogate we obtain the best design with pressure drop of 6612.23 Pa compared to the 6369.11 Pa of original 200 evaluations. This shows the best design depreciated in the approximate model, with a the difference is of 3.8% between these best designs. Similarly for surface uniformity the best design of 200 evaluations stood at 0.9079 , while that of the 1000 evaluation stood at 0.910816, showing an improvement of 0.32%.

The multi objective optimization indicated that both the objective functions are competing against each other. i.e a design with high surface uniformity cannot have a low pressure drop and vice versa. The designs obtained on figure 15 helps designers make this decision related to trade off i.e should a design with better surface uniformity be chosen or better pressure drop for further investigations.

4.1.3 Weighted Sum Objective Parameter Optimization

From previous study of multi objective parameter optimization, the R2 value less than one implies the need of more evaluations[21]. Hence, with the current study, A weighted sum parameter optimization as explained in section 2.4.2, for 250 design evaluation is conducted. The design space with this algorithm reveals not the trade offs between the two observed responses, but an evenly spread out design space. This is inline with the conventional method of optimization where all objectives are assigned individual weights and the resulting solution, like the one seen in the figure, is a weighted sum of all objectives, as discussed from equation 2.43.

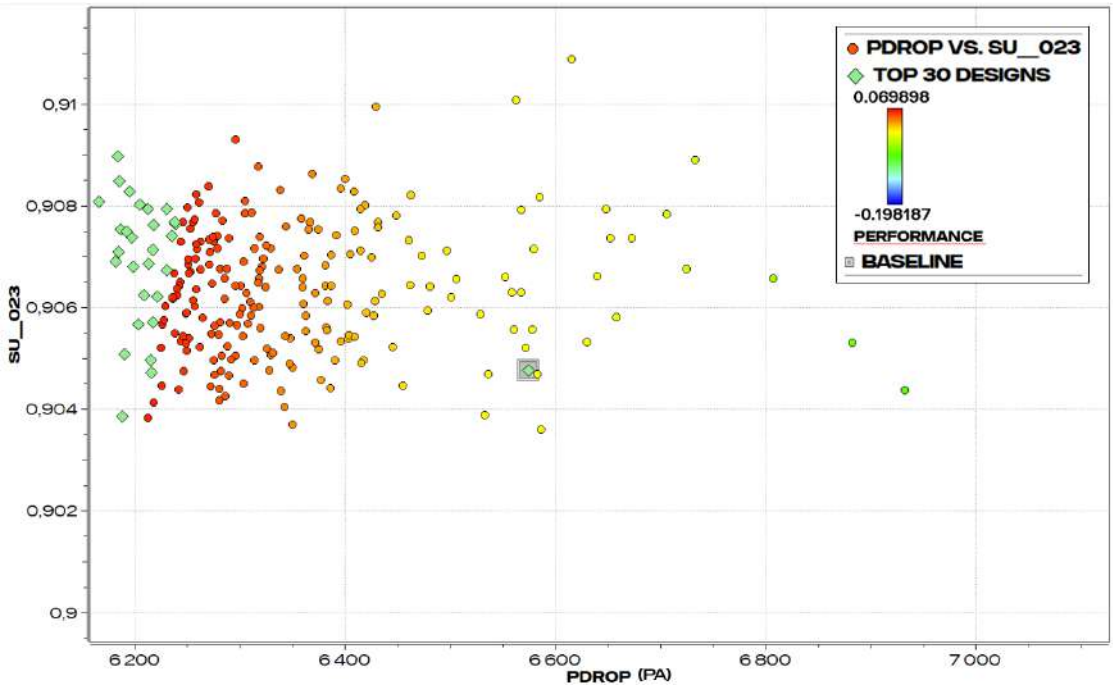

Figure 23: Pareto Plot for weighted sum objective study between pressure drop and surface uniformity

Figure 23 shows the design space for 250 evaluations for weighted sum parameter optimization. Top 30 designs are ranked, as seen in diamonds. Note that these 30 designs will be the subset of the original 250 evaluations, hence they will be originally seen in colored circles too, diamonds are shown just to highlight them.

Unlike figure 15, the designs are not ranked here, as the study is of weighted sum objective. The the best design will be the one with best performance value, minimum pressure drop and maximum uniformity. Again to be observed starting from the most top left corner of the plot.

Figure 24 shows the radial plot of the design space with minimum values towards the center. The colored lines are the non error designs ranked according to the pressure drop. The innermost design in yellow polygon is the best design forming a subset of top 30 designs shown by the range of green region.

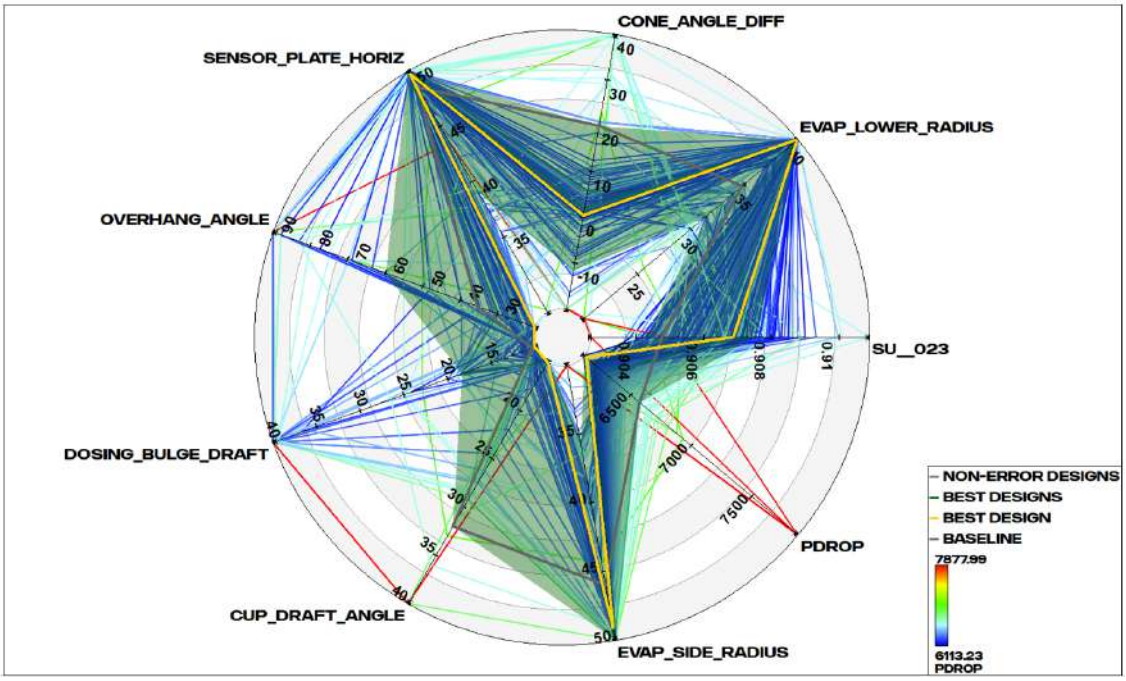

Figure 24: Radial plot for non error with top 30 designs for Weighted sum study.

4.1.3.1 Response surface for Weighted Sum Study

This response modelling is different from previous modelling because it does not involve the complete original design space as the response surfaces of the previous sections did. The current study uses the first 100 design evaluations to approximate the surrogate model. This was done to find insights on developing a similar understanding on the design space, had the run only used 100 evaluations instead of 250. Although usually the designs for the surrogate are separated out based on their Cross Validated Residual values, here, the first 100 designs are selected to understand the approximation, and the closeness with which first 100 evaluations could be used to conduct other studies, based on the surrogate.

Response	Type	Function	Tuning	Shape	R2	RSME	Cross V
SU_023	Kriging	Linear	Gaussian Process	2.01657	0.915	0.00038	0.00129
Pdrop	Kriging	Linear	Gaussian Process	0.102838	0.979	27.4	46.8

Table 5: Response approximation values for Weighted Sum study.

We see with the cross V value for Pressure drop to be slightly better than what was obtained table 3 (46, compared to the previous 130). However, the R2 values for both the responses become less than 1, which implies either the data being noisy, or lack of existing sampling to build an approximation out of it [21]. We also see the shape factor for both the responses to have been decreased, implying that there is some rounded behaviour in the response curve to be expected.

After running many iterations for the cross validation values, the current model, of Kriging with Linear function and a Gaussian tuning process, gave the best cross

Cross V		
SU_023	Value	Difference(%)
Actual min	0.902659	0.143
Actual mean	0.906373	0.143
Actual max	0.910833	0.142

Cross V		
Pdrop(Pa)	Value	Difference(%)
Actual min	6133.23	0.766
Actual mean	6357.32	0.737
Actual max	7877.99	0.594

Table 6: Cross Validation values compared for both objective functions

validation values. The cross Validated residuals for both the responses is plotted against their respective approximate response as follows

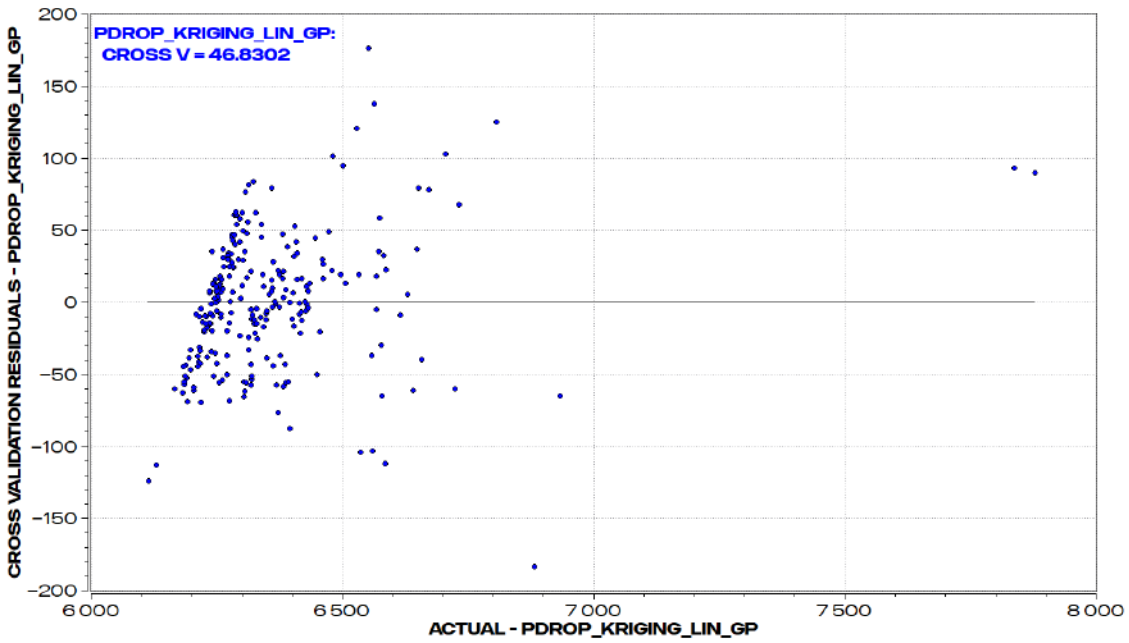

Figure 25: Cross V residuals plotted against kriging response Pressure drop values.

This indicates noise in the data as some of the designs are also lying away from the majority of designs. There is again no symmetric behaviour observed with all the 100 designs used for this approximation. Although this could be the reason why the cross v value of pressure drop reduced from 130 in the Multi objective study, where all 200 designs were used for approximation, to the current 46 value, where only 100 designs are used. This indicates the scope of improvement in building the approximated model, by not selecting all the designs like before. It is also observed that that there remains two such designs for pressure drop, which could appear as outliers.

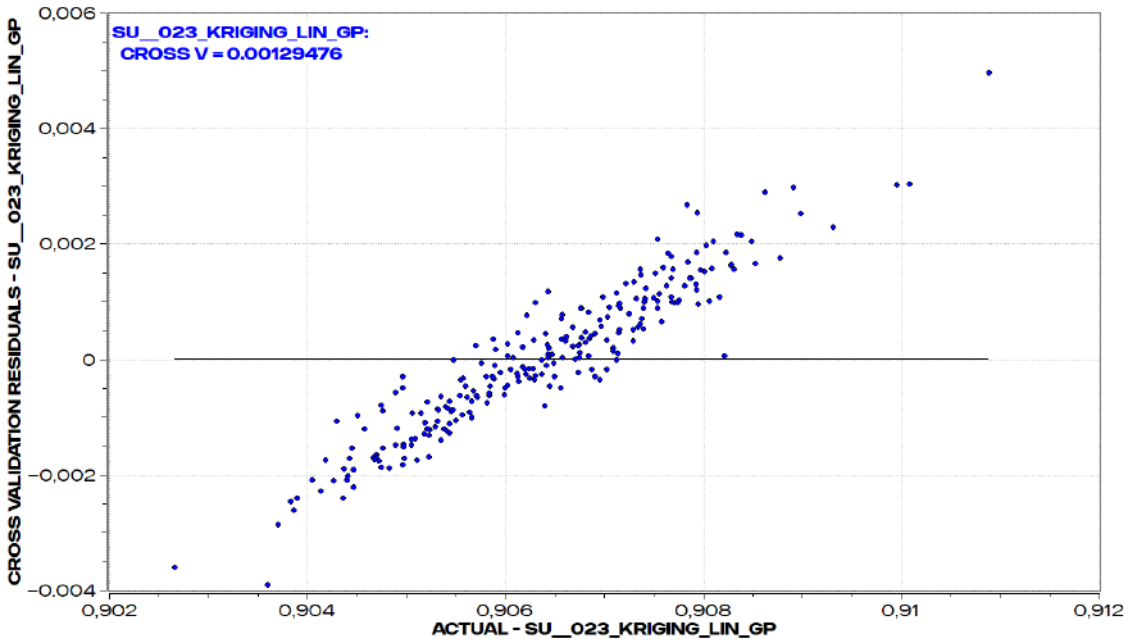

Figure 26: Cross V residuals plotted against obtained kriging response Surface Uniformity values

The Surface uniformity residual, shows again a similar behaviour as per the previously obtained residuals under the same response name. Most of the designs here, also stay with the ± 0.002 limit, indicating a better response surface for the surface uniformity compared to pressure drop. However, the graph is not symmetric indicating lack of goodness of fit as discussed in section 2.4.1.

4.1.3.2 Surrogate for Weighted Sum Study

The cross Validated values, although better than the Multi objective surrogate, still are not without noise. Also, the sampling of 100 designs chosen to approximate the original space, may not approximate the original design space.

Figure 27 shows these responses plotted against each other, with an inset in figure 28 and top 20 designs shown in green diamonds. The performance is again as per the discussion provided in section 2.4.1.

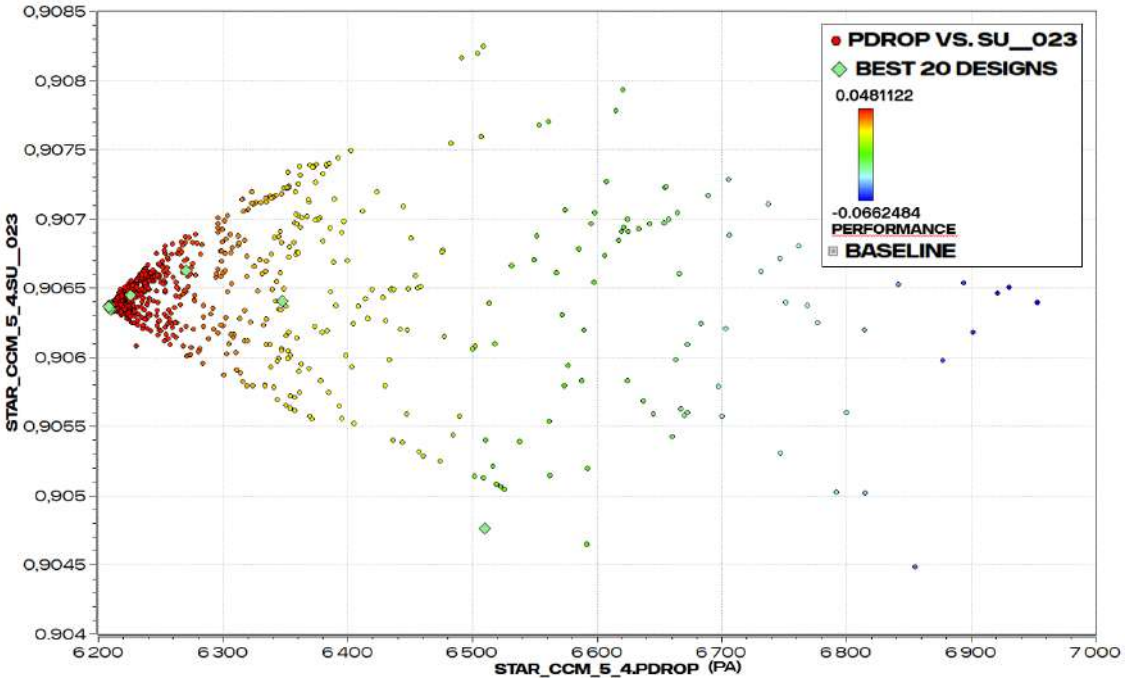

Figure 27: Surrogate for Responses obtained from first 100 design evaluations

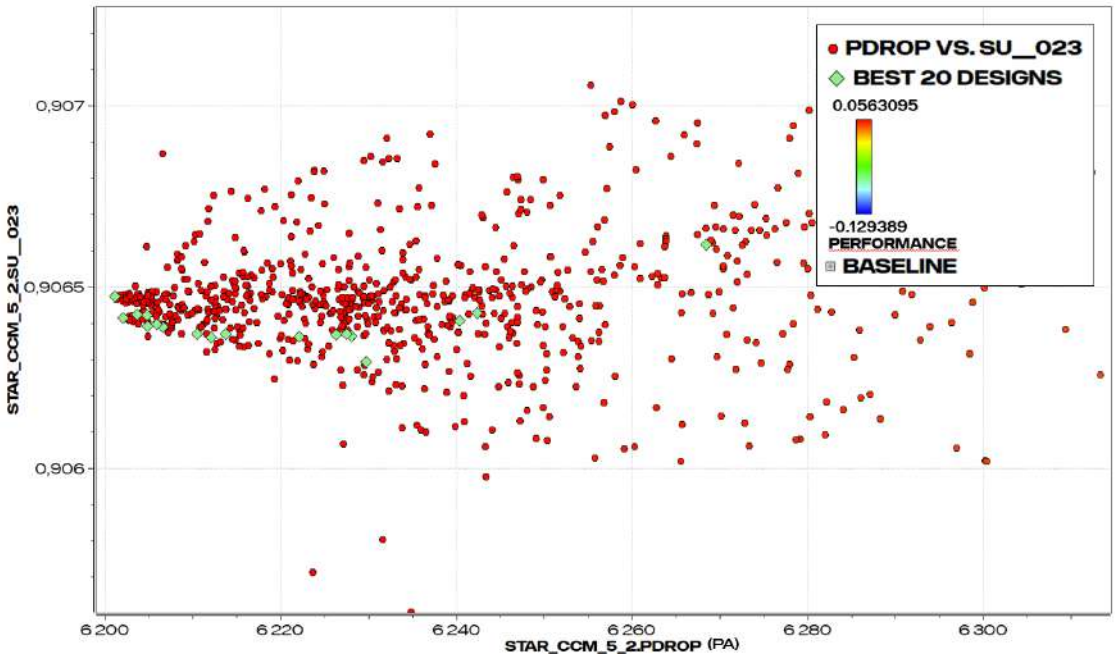

Figure 28: Zoomed inset for the 1000 evaluations

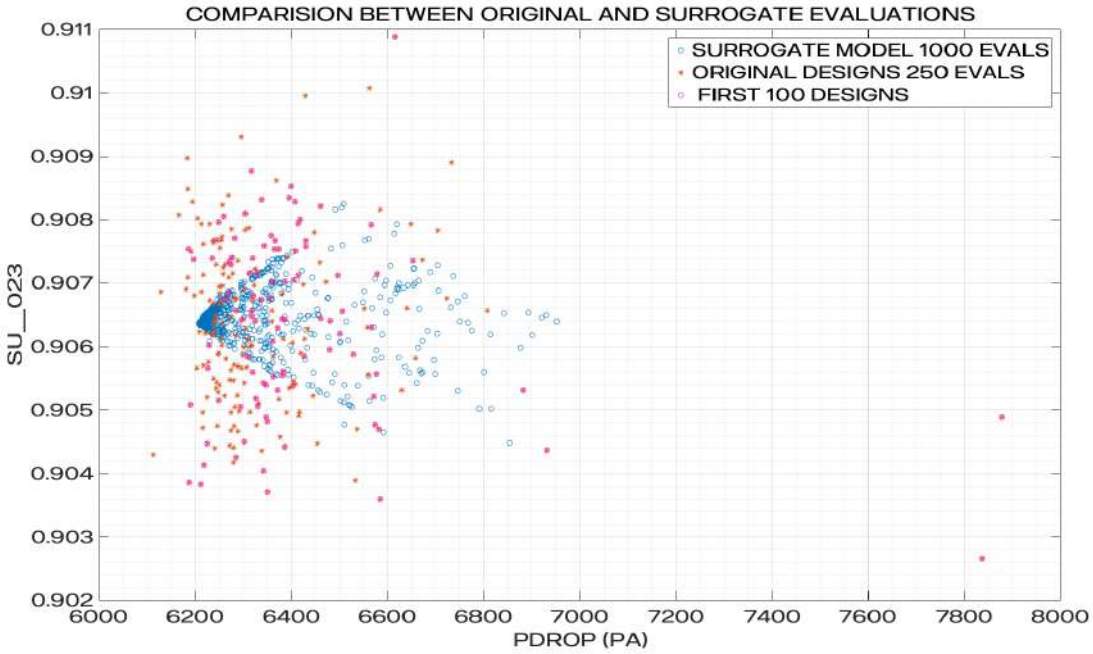

Figure 29: Design space comparison between the 250 and 1000 evaluations highlighted by first 100 evaluations

A comparison is then made between the two design spaces shown in figure 29. It can be seen that the surrogate model, in this case, does not give a better value than the original 250 evaluations. The best design is already obtained from the initial 100 evaluations, indicated by all the pink dots belonging to the top left corner of the plot. The best design for original 250 (and 100) evaluations was at 6129.96 Pa and 0.906869 for surface uniformity, while for 1000 evaluations shown in blue, the best design stood at 6201.1 Pa and 0.906474 for surface uniformity. This is a 1.16% loss of pressure drop and 0.04% loss of surface uniformity. Compared to the baseline of 250 original evaluations Pressure drop showed an improvement of 3.41% and 0.3% for surface uniformity.

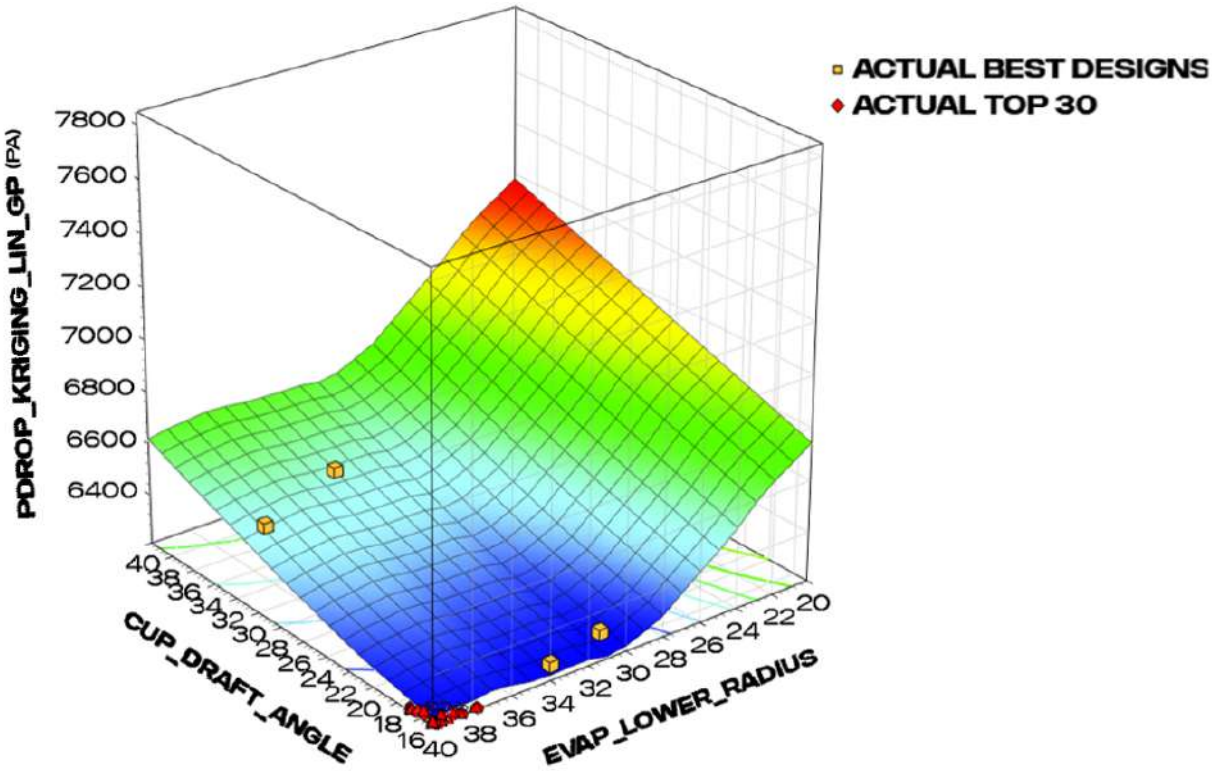

Figure 30: Response surface indicating the global minima with best original 30 designs

A 3D response surface is obtained at the best design obtained from the surrogate, indicating the presence of global minima of the curve. Selected on the two axis are parameters found to have a higher correlation to the response compared to the other parameters, and hence were chosen for this surface. Another important conclusion to corroborate from this surface is the fact that the top 30 designs from the original 250 evaluations are also in this region of global minima (indicated by the valley of curve) for the objective response of pressure drop obtained from the approximation. The golden dots represent the best designs of the approximation, which are relatively far from the global minima.

4.1.4 Verification

Until now, parameters were defined and responses were studied. In this section reverse is done, to observe how well the obtained surrogates perform when the responses are used to retrieve the parameters. A comparison is hence performed with simulating the best designs obtained from the following studies.

- Response surface for Multi Objective Study with 1000 evaluations (section 4.1.2.1).
- Response surface for Weighted Sum Study with 1000 evaluations (section 4.1.3.1).

Their respective best designs are retrieved, then their parameters are plugged into the CAD model used. This is now simulated to verify the surrogate models result separately. As shown with the following, table 7 and table 8

MO	RSM Value	Simulated Value	Obtained Difference(%)	RSM suggested Difference (%)
Pdrop(Pa)	6612.23	6422	-2.96	1.91
SU	0.910816	0.911641	0.090	0.205

Table 7: Best design of Surrogate, simulated from the best responses for multi objective parameter optimization study

WS	RSM Value	Simulated Value	Obtained Difference(%)	RSM suggested Difference (%)
Pdrop(Pa)	6201.1	6341.28	2.21	0.737
SU	0.906474	0.907626	0.12	0.143

Table 8: Best design of Surrogate, simulated from the best responses for Weighted Sum parameter optimization study

We find, for both multi objective (MO) and Weighted Sum (WS) study, the simulated value and the values obtained from response surface are much better for surface uniformity. This trend is completely different in case of pressure drop for both studies. Note that, while building the response surface, HEEDS too calculates this difference, which is shown by RSM suggested difference column.

Although the results seems to be fairly, close, it should be noted that in terms of optimization these are still significant errors. Hence the results are not really usable. However the model is useful, because a desired response was used to get the parameters for the CAD model.

4.2 Spray CFD with AVL FIRE

For spray simulations conducted with AVL FIRE™, 3 objectives are studied in order to find optimal design factoring in all three competing objectives. The response that is separate from previous study, and specific to AVL FIRE™ is the Total Wallfilm mass which is always mentioned in kilogram and is usually in orders of 10^{-4} kg.

The design was conducted for 58 evaluations due to the high resource requirement for the current study. (Note for a complex spray phenomena, 58 is few and more evaluations ought to be conducted.)

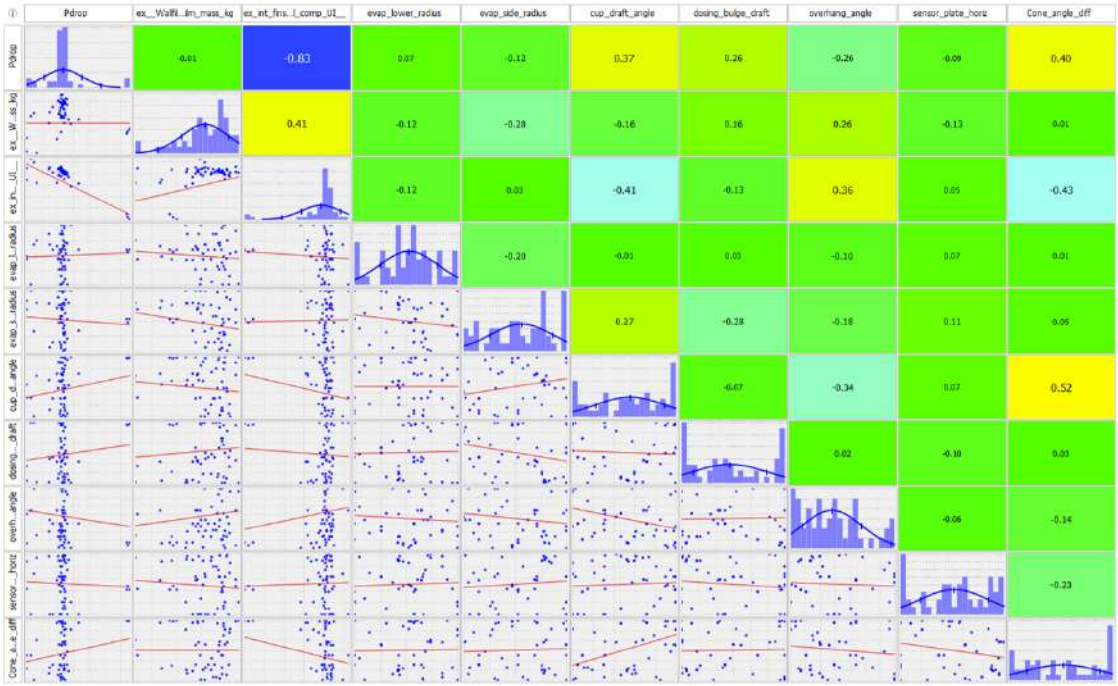

Figure 31: Correlation plot for AVL-FIRE™ study

Figure 31 shows the three objective functions that are defined in the first 3 columns, of this correlation plot, namely, Pressure Drop (Pdrop), Wall film mass (ex_wallfilm_total_film_mass_kg), and Surface Uniformity (ex_int_fins_velocity _component_UI). The other 7 columns form the parameters that build this design space.

Another valuable insight to observe from this plot is that the 2 objective functions, are themselves correlated. This is obtained from the dark blue cell, (cell 2,1 or 1,2) indicating a value of negative 0.83. This indicates decreasing pressure drop would increase the surface uniformity for this study, and vice versa. Similarly, there seems to be also a correlation between wall film mass and uniformity index observed from cell directly under the dark blue cell, (or cell 3,2).

It is observed that just like the DOE study, Cup draft angle and Cone angle difference seems to affect the surface uniformity, yet again, seen in sky blue color and its corresponding symmetric cell.

4.2.1 Multi Objective Parameter Optimization

The three objectives are now studied in combination of two, ranked with the remaining 3rd objective as follows.

- Pressure drop Vs Wallfilm mass ranked with surface uniformity.

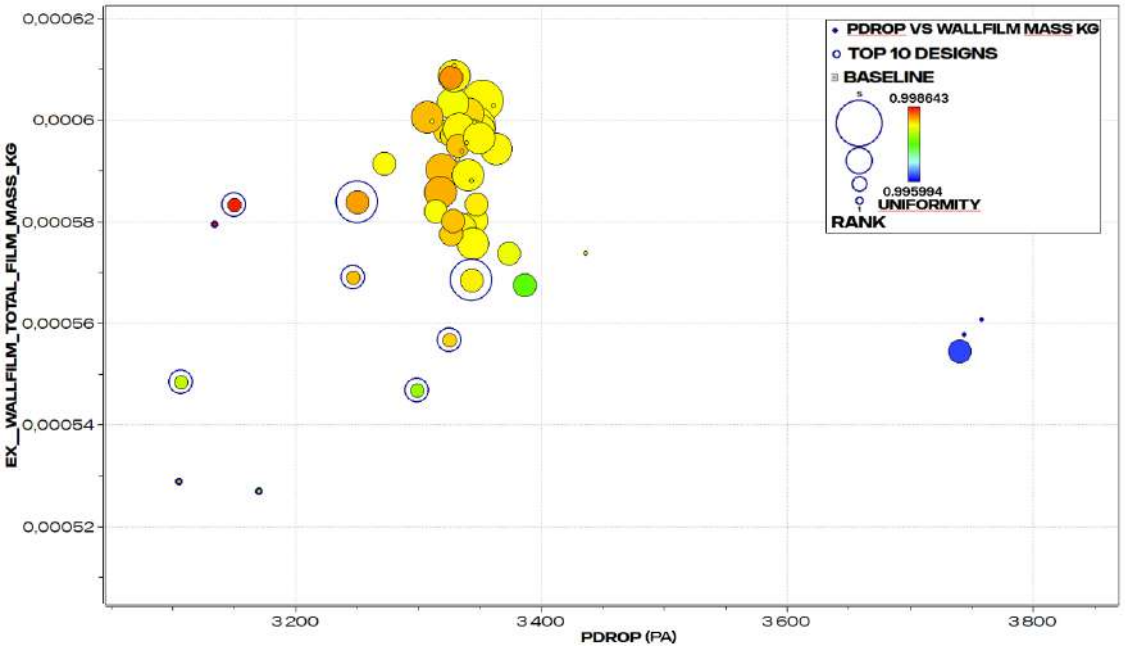

Figure 32: Pressure Drop plotted against Wallfilm mass ranked with Surface uniformity

As the required wall film mass objective is defined to be minimized along with the pressure drop. The ideal region for this graphs will be the designs in the lower left corner of the plot, where two such designs were obtained. The designs are then ranked on their performance number based on the third objective of Surface uniformity. Essentially, this is done simply, to include the data from the third objective with the already present 2 objective on the axis. We see that the rank dimension is much more understandable than in figure 15, this is because in this case, the best designs and not so good designs can be seen localized in different region. This was not the case in the figure 15. Top 10 designs are indicated in the concentric blue circles, with only 2 designs forming the part of so called pareto front.

A response surface with 1000 evaluations is plotted with the original 58 evaluations for Pressure drop Vs Wallfilm mass shown in figure 33. This showcases the region where most of the original evaluations (brown) do not exist and hence giving majority of designs other the original space. Although the behaviour of the sampling seems erratic, it is also quite possible that there must be some outliers, present in the original sampling. The figure forms a zoomed inset to previous figure, such that the last two blue dots present in figure 32, are excluded from the plot.

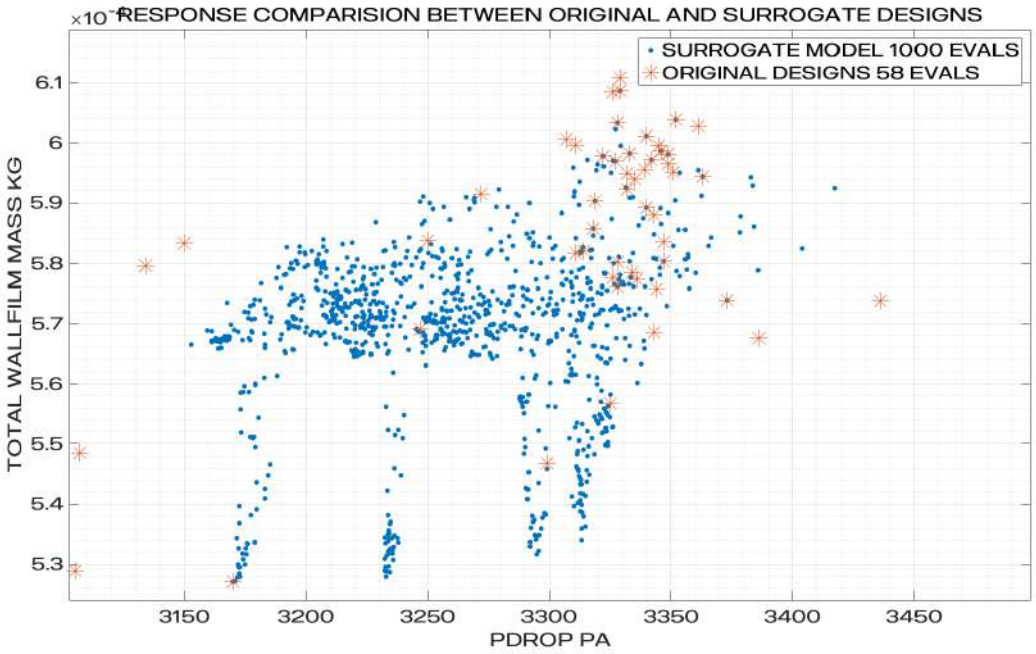

Figure 33: Pressure Drop plotted against Wallfilm mass with the surrogate response

- Pressure drop Vs Surface Uniformity ranked with wall film mass

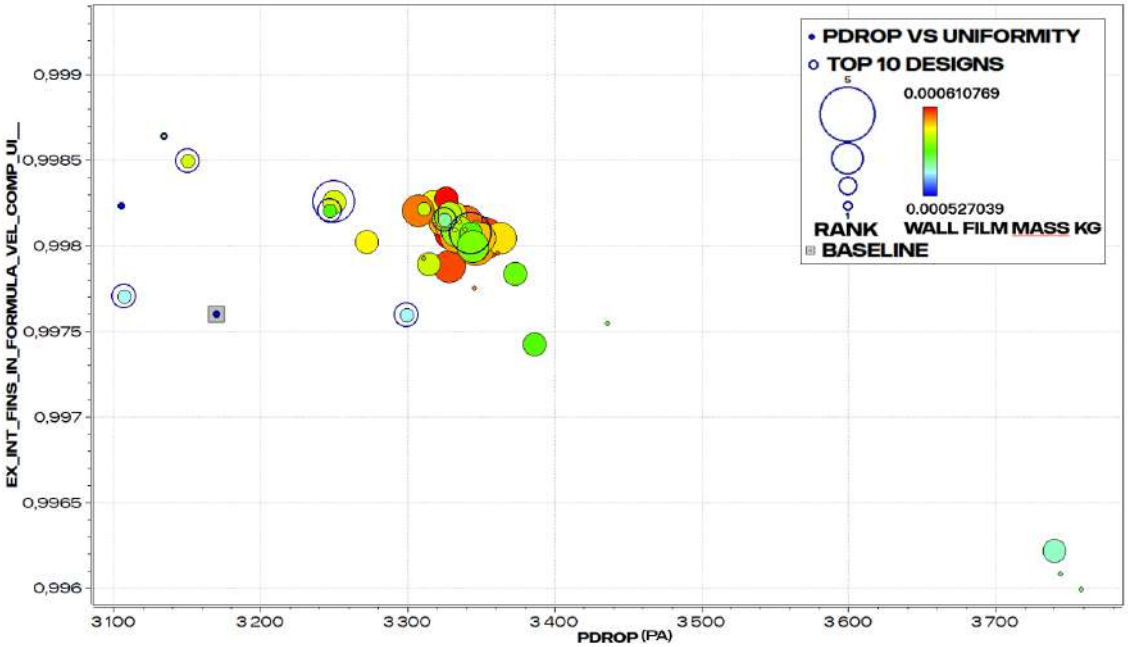

Figure 34: Pressure Drop plotted against Surface uniformity ranked with wall film mass

Figure 34 shows this distribution. In this case, the objective function of surface

uniformity should be maximum while, pressure drop should be minimum, hence the desired region to be is the top left corner of the plot. The approach could also be made towards minimizing pressure drop, this is done by connecting the smallest dots available in the x direction. Similarly, if surface uniformity it to be optimized, the smallest dots are connected towards the y-axis of this plot, in order to obtain the optimal design.

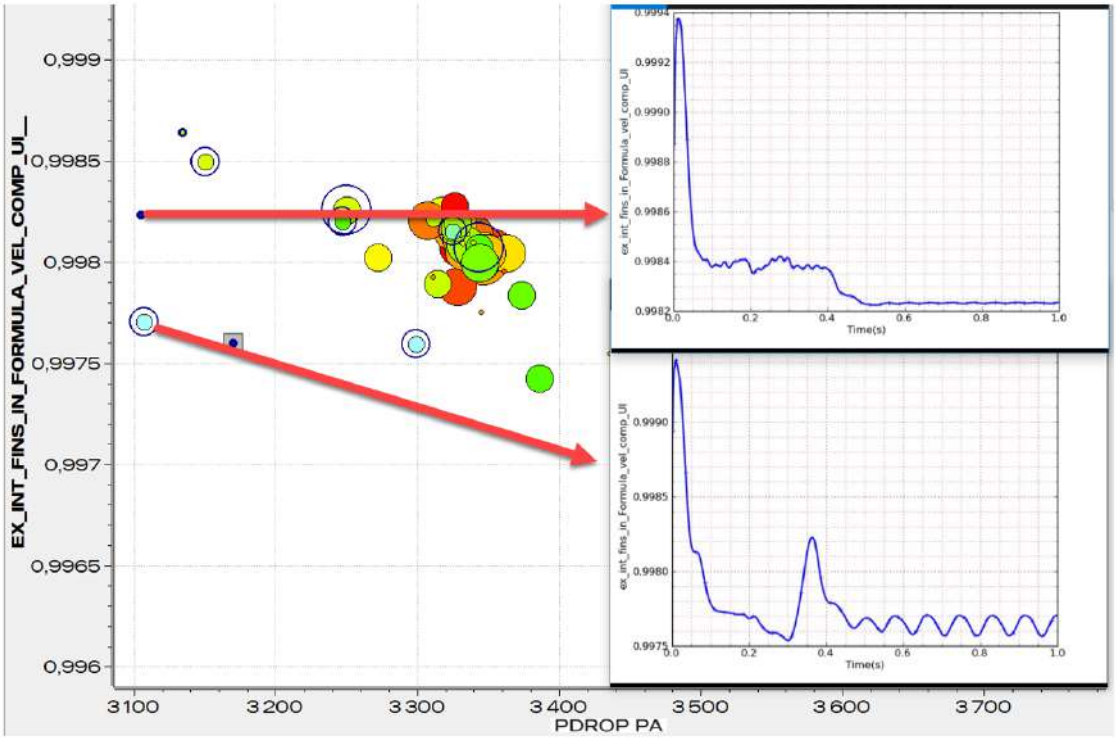

Figure 35: Inset of figure 34 indicating the Uniformity index of two designs out of the 58

Figure 35 shows how the comparison between the uniformity of two designs is made. obtained from python scripts. Here we see that for the spray simulation conducted for 1 s, we see the uniformity in the upper image is converged, but that does not seems to be the case, in the lower image. Hence the upper image of figure 35 is assigned a better rank than the design of the lower image of the same. Similarly, other related insights regarding the objectives under the study could be retrieved, for any of the designs.

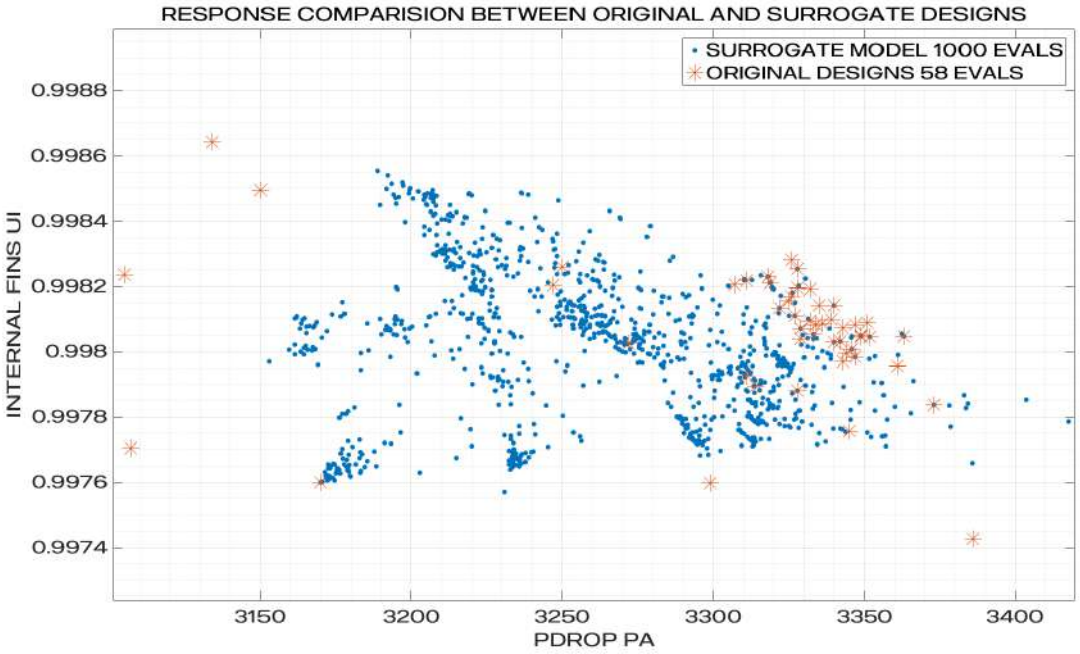

Figure 36: Pressure Drop plotted against surface uniformity with the surrogate response

The approximated space for these two objectives is shown in figure 36. Here, it is observed that the majority of the approximated designs are already in the low pressure drop region than the original design space shown in brown, along with many high surface uniformity designs than the original 4 designs indicated in the left most region in brown, but within a small margin of 3000 Pa and 3150 Pa. However, it does not indicate a better performing region than it's base designs used to build this approximation.

- Wallfilm mass Vs Surface Uniformity ranked with pressure drop.

Figure 37 here shows that the surface uniformity (y-axis) should be maximized while the wall film mass (x-axis) should be minimized. Hence the two dots shown at the leftmost corner of the plot becomes the best designs. We observe that ranks are also assigned with random localization of the size and a small offset in the objective direction is leading to to a drastic change to the rank of the designs.

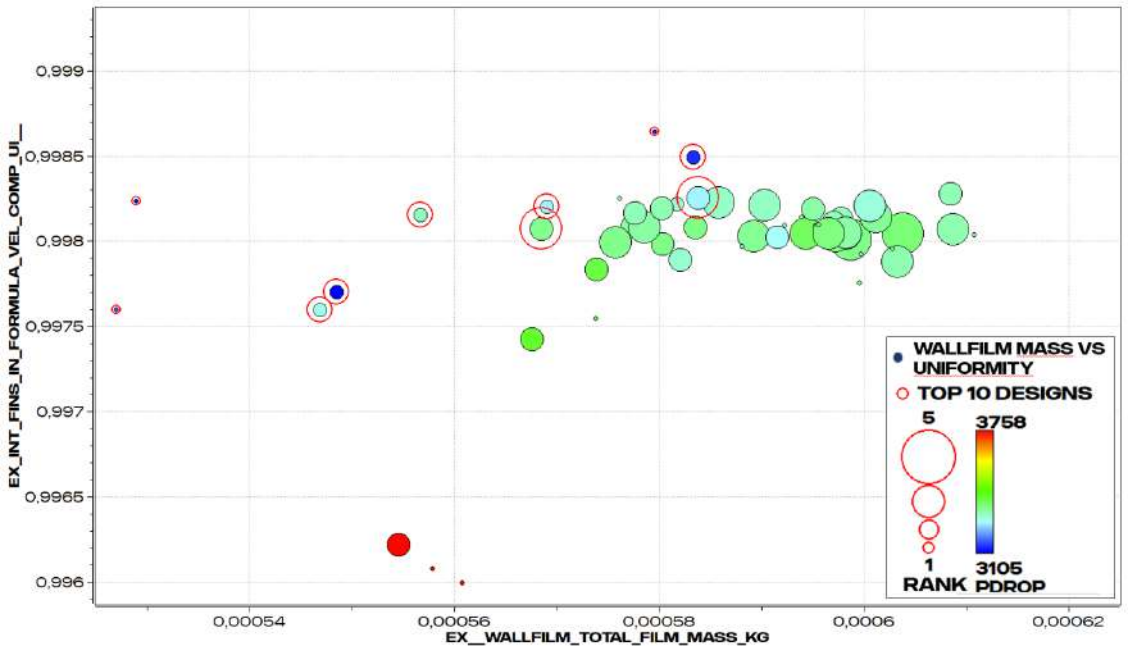

Figure 37: Wallfilm mass plotted against Surface Uniformity ranked with pressure drop

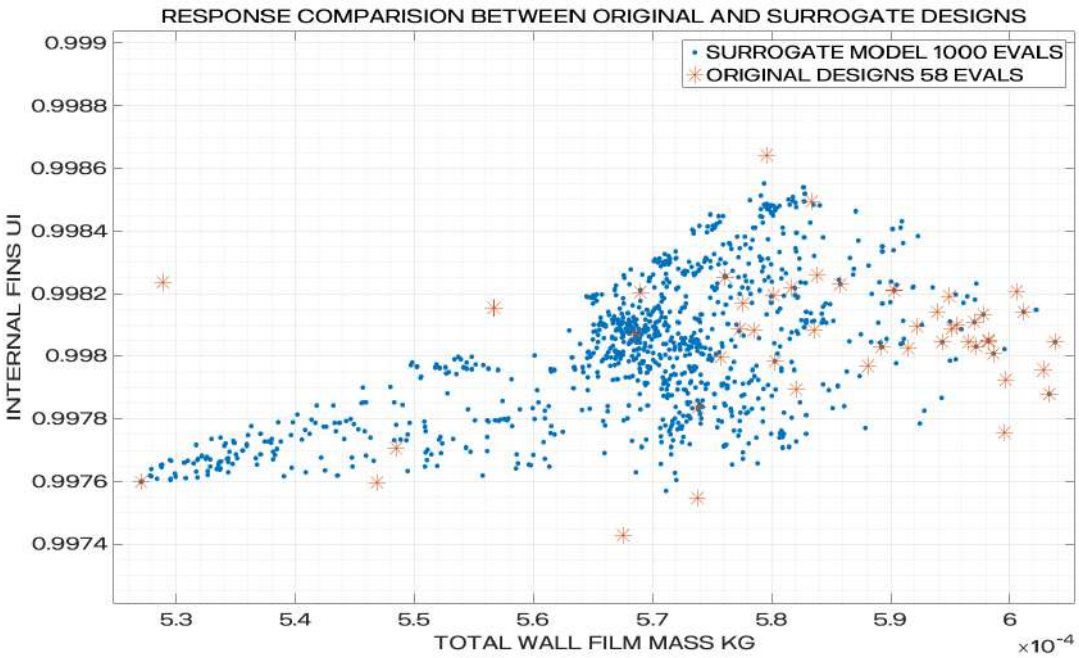

Figure 38: Wallfilm mass plotted against surface uniformity with the surrogate response

The approximated space for these two objectives is shown with figure 38 as follows.

This indicates few designs which are not relatively better in either of the two objective functions, as increasing surface uniformity, will lead to increase of wall film mass too. In a similar fashion, there are few designs which have a better wall film mass, but, do not have a better surface uniformity than the original best surface uniformity.

To conclude, the multi objective parameter optimization for for spray simulations took on average 2 hours per design , hence this was a fairly high resource intensive simulation. The three objectives studied were competing in nature, and indicated 2 such best designs from the current number of evaluations. However, neither of the approximations for this study revealed a better approximation region improving on the original space obtained.

Chapter 5

Conclusions

In the current scope of the Master thesis, an optimization problem, for an aftertreatment exhaust sub system has been conducted. This includes a brief about setting up such a study as well as results obtained from conducting such studies. An aftertreatment Exhaust System used in this study, is currently under development at Scania for it's next generation vehicles and services.

Results are presented from 3 different types of studies available within HEEDS, which is used as an Optimization software at Scania. A simple DoE with one objective response indicated towards scope of improvement for the response. This also showed the parameters that were most affecting this response. Adding another objective as well as a parameter to this study evaluated for more numbers of evaluations with A Multi objective optimization revealed a competing nature of the two objectives, with slight decrease in performance from the base line. Increasing more number of evaluations with a different optimization method gave a best design out of the three methods used. This is summed up in the following table concerning only original evaluations.

STAR-CCM+	Best Pdrop	Best SU
DoE 50 Evals	NA	0.912095
MO 200 Evals	6369.115	0.907965
WS 250 Evals	6183.957	0.906869

Table 9: Comparison of best designs from original evaluations of 3 optimization methods

Here we see an expected trend that a better design in terms of pressure drop was found if there are more number of evaluations are conducted, indicated by the WS250 values. The surface uniformity however, marginally decreases by a factor of 0.12%.

There is a vast decrement in the SU value from DoE to Multi Objective 200 study, because both pressure drop and one additional parameter was added to the Multi Objective Study 200 study from the DoE50 study.

Furthermore, keeping in mind the necessity of building quick understanding of the EAS system for its development as well as the design space constructed from


it, the response surfaces methods have been explored to some extent in order to aid this process of understanding and building other experiments around it.

A Design of Experiments, and an surrogate build from it, illustrate the fact that, with Kriging surrogates, a new design space can be obtained based from only few evaluations. The surrogate was able to predict a region which showed a scope of improvement for the objective function along with indicating which parameters affected it the most.

This however, was not the case, when another objective function of pressure drop was added to the same study along with an added parameter and evaluated for more number of evaluations with the Multi objective study. The response surface did not perform well, or indicate any better design space than the original evaluated space. However, the approximate results, were close under 2% of margin of error. This performance is attributed to the data, that was used without any seclusion of original designs to form the approximated space.

Similarly, for the Weighted sum study, a different HEEDS optimization approach was used, and a slightly higher number of evaluations were conducted with 250 evaluations. This too did not seem to give a better design space than the original evaluated space, when the designs used to build the approximation were only the first 100 designs.

For spray simulations, a simple 58 evaluations in HEEDS with AVL-FIRE™ was conducted involving 3 objective functions along with building a similar response surface for the same. Here, as the sample space was already very less, for a complicated physics phenomena of spray. So, it stands to reason that conducting more number of evaluations will help to build a better approximated surface as is shown by [30].

It appears, as conducting a Design of Experiments with one objective function in mind(not defined), with as many as parameters possible, for only few iterations, could give a better approximated surface. This is also combining the fact that the objective studied was Surface uniformity (between 0 to 1), while it's cross validated residual values will also remain fairly close to zero. When the meta model is built, the Cross V essentially gives an accuracy of the approximation by obtaining these residual values. Adding an objective of pressure drop and another parameter, to this study, decreased the performance of the meta model, also because both of them are of competing nature. This was corroborated from the pareto plot of multi objective study. (figure 15). Hence, the error in the surrogate model made it infeasible to use this as a model for other experiments. More number of evaluations should be conducted, or an approximated model should be build using designs that give an appropriate cross validated residuals and are the subset of the original evaluations.

Although the design spaces could be explored in depth with RSM models, by changing the designs from the original samples, or using only those designs that are already in the required region of the objective function, the emphasis was also on to demonstrating and building a knowledge base for Scania that such an optimization studies is possible within HEEDS to perhaps aid in it's development time for a

product life cycle.

A reverse process of obtaining the parameters from the desired responses of surface uniformity and pressure drop also indicated a new approach to finding the optimal design.

5.1 Future Work

As for further recommendations, there are quite a few possibilities

- Similar studies, can be conducting involving objective functions from other departments apart from NXPS. For example, noise vibration and harshness studies, crash worthiness studies, Acoustic simulations, FEM analysis for acceleration loads and thermal loads, along with the present CFD studies etc, to be included in one workflow itself.
- The response surfaces, could be verified and validated by adding the hardware in the loop analysis (HIL), or software in the loop (SIL), when conducting tests on the test bench, to even reduce the development cycle time. Here the sample objective function, would be the actual test bench values that would be set to maximize or minimize.

Bibliography

[1] UNFCCC. *The Paris Agreement | UNFCCC*. 2000. URL: https://unfccc.int/process-and-meetings/the-paris-agreement/the-paris-agreement (visited on 02/19/2019).

[2] Henrik Bigersson. *Scania Aftertreatment course*. Scania CV AB.

[3] Richard Stone and Palgrave Macmillan. *Introduction to internal combustion engines*. Palgrave Macmillan, 2012.

[4] Mattia Antoniotti. "Optimization of the AdBlue evaporation module for Scania V8 engines". MA thesis. KTH, 2017.

[5] J B Heywood. *Internal combustion engine fundamentals*. New york: Mcgraw-Hill, 1988. ISBN: 9781260116106.

[6] Felix Birkhold et al. "Modeling and simulation of the injection of urea-water-solution for automotive SCR DeNOx-systems". In: *Applied Catalysis B: Environmental* 70 (2007), pp. 119–127.

[7] Guanyu Zheng et al. "Design Optimization of An Integrated SCR System for EU V Heavy Duty Diesel Engines". In: *SAE Technical Paper Series* (2016).

[8] Matthieu Lecompte et al. "The Benefits of Diesel Exhaust Fluid (DEF) Additivation on Urea-Derived Deposits Formation in a Close-Coupled Diesel SCR on Filter Exhaust Line". In: *SAE International Journal of Fuels and Lubricants* 10.3 (Oct. 2017). DOI: 10.4271/2016-01-0945.

[9] Charles Hirsch. *Numerical computation of internal and external flows : fundamentals of computational fluid dynamics*. Elsevier/Butterworth-Heinemann, 2007. ISBN: 9780471923510.

[10] John D Anderson, John F Wendt, and Von Karman. *Computational fluid dynamics : an introduction ; a von Karman Institute book*. Berlin Springer, 1992. ISBN: 9780387534602.

[11] Joel H Ferziger and Milovan Peric. *Computational methods for fluid dynamics*. Springer, 2002. ISBN: 9783540594345.

[12] *STAR-CCM+ Documentation*. Version 13.04. Siemens, 2018.

[13] Herman Weltens et al. "Optimisation of Catalytic Converter Gas Flow Distribution by CFD Prediction". In: *SAE Technical Paper Series* (1993).

[14] *AVL. Spray Module - AVL FIRE® VERSION 2017, edition, v2017.1.* AVL-FIRE™. 2017.

[15] John K. Dukowicz. "A particle-fluid numerical model for liquid sprays". In: *Journal of Computational Physics* 35 (1980), pp. 229–253.

[16] Schiller and AZ Naumann. VDI 77. 1934, pp. 318–320.

[17] Ivanov and V.S. et al. "Spray Penetration and vaporization in Diesel Engines: Numerical Simulation and Experiments". In: *Nonequilibrium Phenomena: Plasma, Combustion, Atmosphere, Moscow, Torus Press* (2009), p. 498.

[18] Kuhnke. D. "Spray Wall Interaction Modeling by Dimensionless Data Analysis". PhD thesis. Technische Universität Darmstadt, 2004.

[19] *AVL. Wallfilm Module - AVL FIRE® VERSION 2017, edition, v2017.1.* AVL-FIRE™. 2017.

[20] *AVL. Thin Wall Module - AVL FIRE® VERSION 2017, edition, v2017.1.* AVL-FIRE™. 2017.

[21] *HEEDS Version 2018.1 Users Manual, 2018.* Siemens. 2018.

[22] *Dakota Version 6.8 Users Manual.* Siemens. 2018.

[23] N Chase, M Rademacher, and E Goodman. *A Benchmark Study of Multi-Objective Optimization Methods.*

[24] Raymond H Myers, Douglas C Montgomery, and Christine M Anderson-Cook. *Response surface methodology : process and product optimization using designed experiments.* Wiley, 2016.

[25] G. G. Wang and S. Shan. *Review of Metamodeling Techniques in Support of Engineering Design Optimization, Journal of Mechanical Design.* Vol. 129. Apr. 2007, p. 370, 2007. DOI: 10.1115/1.2429697.

[26] Noel A C Cressie. *Statistics for spatial data.* John Wiley Sons, Inc, 2015.

[27] Yudong Fang et al. "Automotive Crashworthiness Design Optimization Based on Efficient Global Optimization Method". In: *SAE Technical Paper Series* (2018). DOI: 10.4271/2018-01-1029..

[28] Zhiguang Qian et al. "Building Surrogate Models Based on Detailed and Approximate Simulations". In: *Journal of Mechanical Design* 128 (July 2006), p. 668. DOI: 10.1115/1.2179459.

[29] L. Boussouf. "Surrogate Based Optimization for Multidisciplinary Design". In: *SAE International* (Oct. 2011). DOI: 10.4271/2011-01-2507.

[30] David Ginsbourger et al. "A note on the choice and the estimation of Kriging models for the analysis of deterministic computer experiments". In: *Applied Stochastic Models in Business and Industry* 25 (2009), pp. 115–131.